

# Tumor microenvironment in bone sarcomas: Implications for immunotherapy and emerging therapeutic vulnerabilities (Review)

WENTAO LI, LIJUN LV, YIBIN JIN and XIN YUAN

Department of Orthopedic Surgery, The Third Affiliated Hospital of Gansu University of  
Chinese Medicine, Baiyin, Gansu 730900, P.R. China

Received September 1, 2025; Accepted October 31, 2025

DOI: 10.3892/or.2026.9050

**Abstract.** Bone sarcomas remain lethal despite multimodal therapy, primarily because the mineralized, immunosuppressive tumor microenvironment (TME) promotes chemo- and immune-resistance. Integrating single-cell and spatial omics across osteosarcoma, Ewing sarcoma and chondrosarcoma delineates subtype-specific TME archetypes dominated by M2 macrophages, exhausted T cells and a stiff extracellular matrix. Mechanistic dissection reveals tractable vulnerabilities, myeloid reprogramming, extracellular matrix modulation and metabolic and epigenetic checkpoints, that can be targeted with bone-selective delivery systems and biomarker-driven combination trials to convert therapeutic failure into durable remission. Therefore, the aim of the present review is to synthesize the latest single-cell, spatial and functional data to map bone-sarcoma TME heterogeneity, dissect resistance mechanisms and propose integrated, biomarker-guided therapeutic strategies that can be translated into treatments.

## Contents

1. Introduction
2. Deconstructing the bone sarcoma TME: Cellular and non-cellular
3. Mechanisms of immunosuppression within the bone sarcoma TME
4. Immunotherapy in bone sarcomas: Current landscape and TME-driven challenges

---

*Correspondence to:* Professor Xin Yuan, Department of Orthopedic Surgery, The Third Affiliated Hospital of Gansu University of Chinese Medicine, 222 Silong Road, Baiyin, Gansu 730900, P.R. China  
E-mail: 18893003313@163.com

*Key words:* bone sarcoma, tumor microenvironment, immunotherapy resistance, myeloid reprogramming, extracellular matrix remodeling, single-cell and spatial omics, adoptive cell therapy

5. Therapeutic targeting of the bone sarcoma TME
6. Preclinical models and emerging technologies
7. Future directions and translational challenges
8. Conclusion

## 1. Introduction

Bone sarcomas, osteosarcoma (OS), Ewing sarcoma (ES) and chondrosarcoma (CS), collectively account for 2-3% of all childhood and adolescent types of cancer, yet they remain the third leading cause of cancer-related mortality in patients aged 10-25 years (1). Globocan 2024 reports an annual incidence of 0.3 for OS, 0.2 for ES and 0.4 for CS per 100,000, with no plateau in incidence over the past decade (2). Distal extremity primaries dominate OS and ES, whereas CS arises predominantly in axial locations and is prone to local relapse (2). Genomic heterogeneity is extreme: OS is characterized by TP53/RB1 disruption and chromothripsis, ES by EWSR1-FLI1 translocations and CS by IDH1/2 or COL2A1 mutations, which shape distinct immune landscapes (3,4). This biological diversity translates into variable outcomes, 5-year overall survival is 65-70% for localized OS but decreases to <30% when metastatic (5); ES achieves 75% survival with multimodal therapy but remains <25% after recurrence (6) and high-grade CS shows only 10-15% survival once unresectable (7). Despite their rarity, these tumors impose a disproportionate clinical burden that calls for mechanism-based therapeutic innovation.

Curative intent still hinges on surgery plus multi-agent cytotoxic chemotherapy, with radiation reserved for margin-positive or unresectable disease (8). Neoadjuvant response, defined by  $\geq 90\%$  necrosis, associates with survival, yet 35-45% of patients with OS achieve poor histologic response and carry a 3-fold higher risk of metastatic relapse (8). High-grade CS is intrinsically chemo- and radio-resistant, leaving wide excision as the only curative option, which is often impossible in pelvic or skull-base locations. Dose intensification has reached ceiling toxicity without further survival benefit; therefore, high-risk groups (metastatic presentation, axial primaries or <90% necrosis) urgently require alternative strategies (9). Importantly, traditional regimens neglect the tumor microenvironment (TME), which orchestrates chemoresistance

through hypoxia-induced quiescence, extracellular matrix (ECM)-mediated drug trapping and immunosuppressive cytokines such as TGF- $\beta$  and IL-10. Recognizing these TME-centric escape mechanisms is essential to explain why even aggressive multimodal therapy fails in a substantial subset of patients (10,11).

The bone sarcoma TME is an intricate ecosystem composed of malignant cells interwoven with cancer-associated fibroblasts (CAFs), bone-marrow-derived mesenchymal stromal cells, osteoclasts, endothelial cells and a spectrum of innate and adaptive immune cells (12). Single-cell RNA-sequencing (scRNA-seq) of untreated OS resolved nine major non-malignant populations, including C1Q+ tumor-associated macrophages (TAMs), exhausted CD8+ T cells, regulatory T cells (Tregs) and dysfunctional dendritic cells (DCs) (13). Non-cellular components are equally important: A collagen- and versican-rich ECM increases tissue stiffness, promotes integrin-mediated survival signaling and impedes cytotoxic T-cell infiltration (14). Hypoxia and acidic pH gradients generated by aerobic glycolysis stabilize hypoxia inducible factor (HIF)-1 $\alpha$ , upregulate programmed death-ligand 1 (PD-L1) and skew macrophages toward an M2 immunosuppressive phenotype (15). Dynamic crosstalk between these elements, for example, TAM-derived TGF- $\beta$  induces OS stemness while tumor-secreted CSF-1 reciprocally sustains TAMs survival, creates a self-reinforcing niche that fosters progression and therapy resistance (16,17).

Pre-clinical lineage-tracing studies demonstrate that disseminated OS cells seed the lung as early as diagnosis, but only those that have educated a pre-metastatic niche rich in S100A8/A9+ myeloid cells and ECM crosslinking enzymes successfully colonize (18,19). In ES, CD99-mediated reprogramming of macrophages suppresses antigen presentation, facilitating immune evasion during transit (20). Locally, hypoxia-induced exosomes transfer micro (miR)-135b from tumor cells to endothelial cells, promoting angiogenesis and subsequent osteolysis (21). Chemotherapy itself reshapes the TME: Cisplatin increases M2-TAMs infiltration and PD-L1 expression, whereas doxorubicin enriches ECM cross-linking enzymes, both contributing to acquired resistance (22). Radiation upregulates antigen presentation machinery yet simultaneously expands CD47+ macrophages that blunt T-cell cytotoxicity (23). Thus, the TME not only fuels primary tumor growth but also orchestrates metastatic spread and shields residual cells from cytotoxic, targeted and immune attack, positioning it as the central bottleneck for durable cures.

OS is the most frequent primary malignant bone neoplasm, with a bimodal age distribution encompassing adolescents and the elderly (1,2). Despite aggressive multi-modal therapy, ~40% of patients with OS develop pulmonary metastases within 5 years, and the 5-year survival for metastatic disease remains <30% (5). Single-cell RNA sequencing coupled to intravital imaging has recently shown that invasive osteosarcoma cells heighten focal adhesion kinase/SRC signaling when confronted with extracellular-matrix stiffening (Young's modulus >30 kPa), facilitating amoeboid migration and trans-endothelial extravasation (24). Hypoxia-induced exosomal miR-135b transferred from tumor to endothelial cells enhances vascular endothelial growth factor (VEGF)-independent angiogenesis and osteolysis, facilitating pre-metastatic niche formation

in the lung (21). Additionally, M2-polarized TAMs secrete CCL18, which activates the PI3K/AKT pathway in OS cells and increases MMP9 expression, further augmenting local invasion and intravasation (25). These observations position the TME not only as a barrier to therapy but also as an active driver of metastatic cascade, underscoring the urgency of targeting both tumor-intrinsic and microenvironmental determinants of invasion.

Current regimens yield suboptimal survival in patients with metastatic or relapsed bone sarcomas, partly because cytotoxic protocols overlook the immunosuppressive, mechanically rigid and metabolically hostile TME. Previous publications have summarized individual TME components in OS pathogenesis and discussed therapeutic targets (13-15). This present review extends beyond these earlier reports by integrating scRNA-seq, spatial proteomics and functional imaging across OS, ES and CS to define subtype-specific TME archetypes. In addition, a mechanistic framework that associates mineralized-matrix mechanics, metabolic acidosis and myeloid reprogramming to primary and acquired immunotherapy resistance is presented and biomarker-guided combination strategies are proposed for addressing these challenges.

## 2. Deconstructing the bone sarcoma TME: Cellular and non-cellular

Single-cell atlases and spatial proteomics now resolve OS, Ewing and CS microenvironments into archetypes dominated by M2 macrophages, exhausted CD8+ T cells and stiff collagen-versican ECM. Fig. 1 provides the reference framework for dissecting subtype-specific cellular and non-cellular determinants of immune privilege and drug resistance.

### *Cellular compartments*

*Immune infiltrate.* scRNA-seq has revealed striking inter-tumoral heterogeneity that directly conditions immunotherapy outcomes (26). In OS, CD3+ T cells constitute 8-15% of all viable cells; however, 60-80% of these cells display an exhausted PD-1+ T-cell Immunoglobulin and Mucin-domain containing-3 (TIM-3)+ Lymphocyte Activation Gene 3 (LAG-3)+ phenotype and are spatially confined to the tumor periphery by CXCL12-rich reticular networks (27). By contrast, ES lesions harbor an even lower overall T-cell fraction (2-5%) but a higher CD8+/ Tregs ratio, possibly explaining the 20% objective response rate to pembrolizumab monotherapy observed in the EURO-EWING-2012-NIS trial (NCT 02707557), whereas OS trials have yet to >5% objective response rate (28). These divergent landscapes argue against a 'one-size-fits-all' checkpoint blockade strategy and suggest that CXCR4 or CXCL12 inhibition might preferentially benefit OS by enhancing T-cell trafficking.

Myeloid populations dominate the sarcoma TME across subtypes, yet their functional states are context-dependent (29). In OS, two independent scRNA-seq cohorts (n=11 and n=19) both identified a continuum of TAMs skewed toward M2-like signatures (CD163+CCL18+MMP12+), associating with shorter metastasis-free survival (HR=2.3, P=0.007) (13). Conversely, CS TAMs express higher inducible nitric oxide synthase (iNOS) and tumor necrosis factor- $\alpha$  (TNF- $\alpha$ ), resembling an M1 phenotype, but paradoxically co-express PD-L1 and

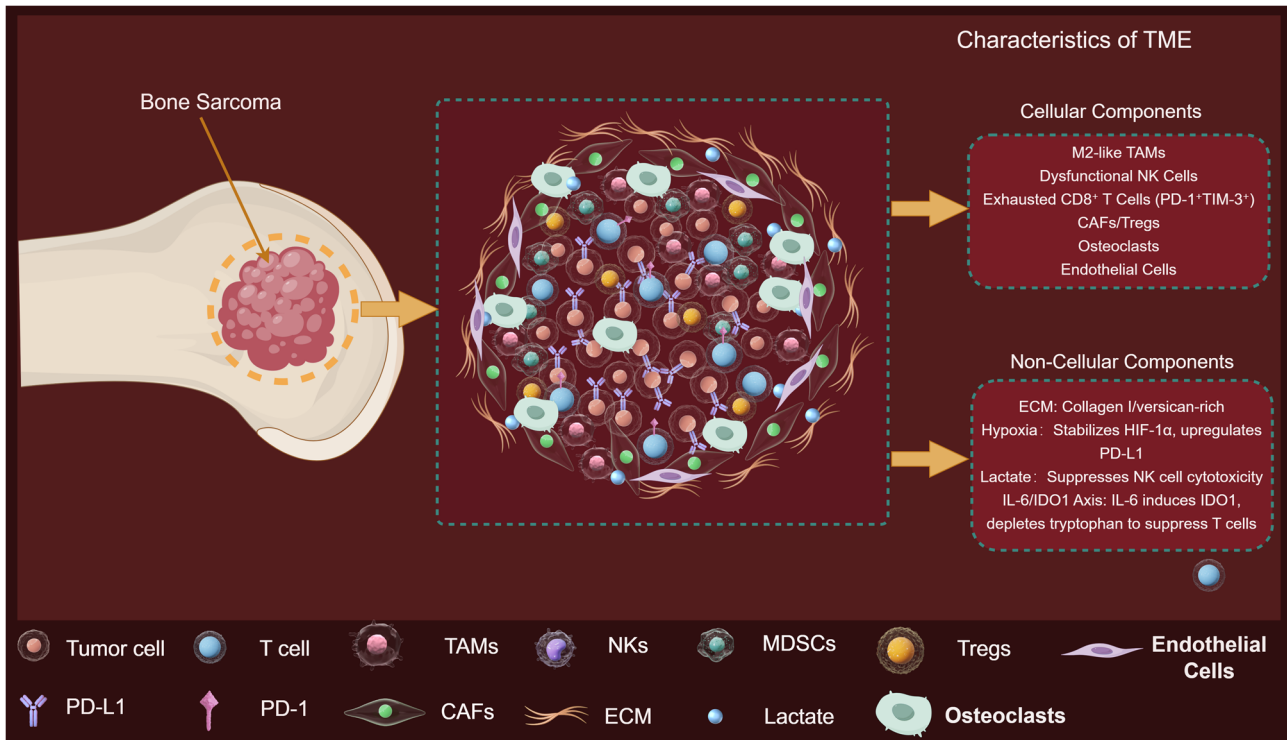


Figure 1. A schematic diagram illustrating the characteristics of the tumor microenvironment in bone sarcoma (figure was created using the online graphic design website Figdraw: [www.figdraw.com](http://www.figdraw.com)). TAM, tumor-associated macrophage; CAF, cancer-associated fibroblast; ECM, extracellular matrix; PD-L1, programmed death-ligand 1; IDO1, indoleamine 2,3-dioxygenase 1; MDSCs, myeloid-derived suppressor cells; NK, natural killer; Tregs, T-regulatory cells; HIF-1 $\alpha$ , hypoxia inducible factor-1 $\alpha$ ; TIM-3, T-cell Immunoglobulin and Mucin-domain containing-3.

indoleamine 2,3-dioxygenase 1 (IDO1), indicating a hybrid state that may blunt anti-PD-1 efficacy despite apparent ‘inflammatory’ polarity (30). These conflicting data underscore the need for multi-omic spatial mapping to resolve whether M1/M2 classifications are sufficient biomarkers in bone sarcomas.

Myeloid-derived suppressor cells (MDSCs) and regulatory DCs further entrench immunosuppression. In canine OS, PMN-MDSCs rise from <3% in healthy marrow to 18% within tumor tissue and their depletion with PI3K $\delta$  inhibitor GS-9820 restores antigen-specific T-cell proliferation *ex vivo* (31). A separate study reported that conventional DC1s are virtually absent in 70% of high-grade CS specimens, and forced re-introduction of FLT3L-matured DC1s in patient-derived organoids re-sensitized tumors to  $\gamma\delta$  T-cell killing (32). Collectively, these findings position combinatorial regimens that simultaneously deplete MDSCs and replenish DC1s as a rational next step for clinical testing.

Natural killer cells (NKs) abundance is high in ES (<12%), but their cytotoxicity is crippled by transforming growth factor- $\beta$ 1 (TGF- $\beta$ 1) concentrations >800 pg/ml, levels that exceed those in OS by 3-fold (33). Blockade of TGF- $\beta$ RI with galunisertib restored NKs degranulation against ES cell lines *in vitro*, providing a mechanistic rationale for the ongoing phase I/II trial of galunisertib plus dinutuximab  $\beta$  (NCT05461567) (34).

**Stromal cells.** CAFs originate from resident bone-marrow mesenchymal stem cells (MSCs) and adopt heterogeneous phenotypes. CAFs constitute a dominant stromal component in bone sarcomas and are increasingly recognized as co-architects of the immunosuppressive niche (35). scRNA-seq of

human OS biopsies resolved two transcriptionally stable CAF subsets-myofibroblastic CAFs (myCAFs, ACTA2<sup>high</sup>) and inflammatory CAFs (iCAFs, IL-6<sup>high</sup>CXCL12<sup>high</sup>), that together account for 25-35% of all non-malignant cells (35). Lineage-tracing studies in genetically engineered mouse models indicate that the majority of CAFs arise from local bone-marrow-derived mesenchymal stromal/stem cells (BM-MSCs) through TGF- $\beta$ - and bone morphogenetic protein-2 (BMP-2)-driven reprogramming, a process that is molecularly indistinguishable from the osteoblastic differentiation cascade that gives rise to the malignant clone itself (35). Consequently, OS cells and CAFs share an overlapping mesenchymal developmental program, including expression of platelet-derived growth factor receptor (PDGFR)- $\beta$ , CD90 and the osteoblastic transcription factor RUNX2, suggesting that the same oncogenic cues that initiate the tumor concurrently instruct CAF fate. This ontological convergence explains why CAFs are uniquely equipped to deposit a collagen- and versican-rich ECM that matches the stiffness (Young’s modulus 25-35 kPa) of the surrounding mineralized bone, thereby shielding tumor cells from immune attack and impeding chimeric antigen receptor T-cell (CAR-T) cell penetration (36). Two transcriptionally distinct CAF subpopulations have been delineated: myCAFs (ACTA2<sup>high</sup>) and iCAFs (IL-6<sup>high</sup> CXCL12<sup>high</sup>) (37). In OS, myCAFs aligned along collagen bundles associate with increased tissue stiffness (Young’s modulus 25-35 kPa) and impaired CAR-T penetration, whereas iCAFs secrete CXCL12 that recruits CXCR4<sup>+</sup> Tregs (38). Targeting CXCL12 with plerixafor sensitized OS xenografts to disialoganglioside 2 (GD2). CAR-T therapy, increasing intratumoral CAR-T

density 4-fold (39). These data highlight CAFs subtyping as a prerequisite for effective stromal reprogramming.

Osteoblast-lineage cells, often dismissed as bystanders, actively shape immune privilege (40). Single-cell interactome analyses revealed 21 ligand-receptor pairs between OS cells and osteoblasts, including RANKL-RANK and Jagged1-Notch2 axes that polarize macrophages toward an M2 phenotype and upregulate PD-L1 (41). Pharmacologic RANKL inhibition with denosumab not only reduced osteoclastogenesis but also decreased M2-TAMs abundance by 40% in a syngeneic OS model, suggesting dual anti-resorptive and immunomodulatory benefits (42). Conversely, osteoclasts fuel a vicious cycle of bone destruction and TGF- $\beta$  release; TGF- $\beta$  concentrations >1 ng/ml were sufficient to convert 50% of CD8+ T cells into FOXP3+ Tregs in Transwell assays (43). These observations position osteoclast-directed therapy as a combinatorial partner for TGF- $\beta$  inhibition.

**Endothelial cells and angiogenesis.** Bone sarcomas develop a chaotic vasculature characterized by tortuous, CD31-high and NG2-low vessels with poor pericyte coverage (44). Microvessel density is highest in ES (mean 104 vessels mm<sup>-2</sup>) and lowest in CS (42 vessels mm<sup>-2</sup>), paralleling VEGF-A expression levels (45). Yet, bevacizumab achieved only modest disease stabilization [6-month progression-free survival (PFS) 18%] in a phase II OS trial, possibly because VEGF blockade paradoxically increased hypoxia and HIF-1 $\alpha$ -driven PD-L1 expression on tumor cells (46). Alternative strategies that normalize rather than prune vessels, such as low-dose metronomic cyclophosphamide enhanced CART cells infiltration in murine ES models without exacerbating hypoxia, underscoring the need to balance anti-angiogenic and immunotherapeutic dosing schedules (47).

**MSCs.** MSCs are recruited to primary tumors via CCL5-CCR5 signaling and differentiate into either CAFs or osteoblast-like cells depending on TGF- $\beta$  and BMP-2 gradients (48). In OS, MSCs-secreted PGE2 induces IDO1 in DCs, leading to a 60% reduction in T-cell proliferation in mixed lymphocyte reactions (49). Genetic ablation of cyclooxygenase-2 (COX-2) in MSCs restored DCs function and improved anti-PD-1 efficacy *in vivo* (50). These findings suggest that MSCs-educated immune suppression is reversible and that COX-2 inhibition could serve as an adjuvant to checkpoint blockade.

In summary, osteoblast-lineage cells, osteoclasts, MSCs and endothelial cells each contribute distinct immunosuppressive cues, including cytokine secretion, ECM remodeling, and metabolic reprogramming. These interactions not only reinforce tumor survival but also impede effective immune surveillance. A summary of key bone-related cells, their ontogeny, immunosuppressive mediators, and therapeutic implications is presented in Table I (14,34,42,47,50), highlighting potential targets for microenvironment-directed interventions.

#### *Non-cellular compartments*

**ECM.** The bone sarcoma ECM is a composite of type-I collagen, hydroxyapatite nanocrystals and oncofetal fibronectin (51). Atomic-force microscopy shows that OS ECM stiffness (10-40 kPa) is 3-fold higher than adjacent marrow, a mechanical cue that activates yes-associated protein

(YAP)/transcriptional co-activator with PDZ-binding motif (TAZ) and downregulates MHC-I in tumor cells (52). Lysyl oxidase-like 2 (LOXL2)-mediated collagen cross-linking is elevated in metastatic bone sarcomas and targeting LOXL2 improves both chemotherapeutic drug delivery and the efficacy of adoptive T-cell therapies (14).

**Soluble factors.** Multiplex cytokine profiling of OS biopsies identified a high-TGF- $\beta$ /low-interferon- $\gamma$  (IFN- $\gamma$ ) signature that independently predicted poor histologic response to neoadjuvant MAP chemotherapy (53). Tumor-derived IL-6 and CXCL12 establish an autocrine/paracrine loop that recruits CXCR4+ MDSCs and polarizes macrophages to an M2 phenotype (54). These soluble factors collectively sculpt an immunosuppressive milieu and establish the rationale for co-targeting IL-6, CXCL12 and TGF- $\beta$  in combination regimens.

**Hypoxia.** Hypoxia (pO<sub>2</sub> <10 mmHg) affects 40% of OS and 60% of ES lesions, driving HIF-1 $\alpha$  stabilization and downstream glycolytic reprogramming (55). A meta-analysis of 487 patients with OS associated elevated HIF-1 $\alpha$  to a 2.1-fold increased risk of metastasis. While HIF-1 $\alpha$  knock-down radiosensitizes OS cells, it simultaneously upregulates PD-L1, implying that radiation-HIF-1 $\alpha$ -PD-L1 combinations warrant evaluation (56). Hypoxia-activated prodrugs such as TH-302 demonstrated modest single-agent activity (disease control rate 28%), but when combined with anti-cytotoxic T-lymphocyte associated protein 4 (CTLA-4), metastatic lung lesions shrank by 50% in a murine ES model (55).

**Acidosis and nutrient deprivation.** Lactate concentrations >15 mM in OS interstitial fluid, suppressing NKs cytotoxicity by 50% via GPR81-dependent mechanisms (57). Pharmacologic buffering with oral sodium bicarbonate restored NK function and improved anti-GD2 antibody efficacy *in vivo*, supporting a readily translatable adjunct (58). Pharmacologic buffering with oral sodium bicarbonate restored NK cytotoxicity and enhanced anti-GD2 antibody efficacy in orthotopic OS models, confirming rapid translatability of this metabolic adjunct (58).

### **3. Mechanisms of immunosuppression within the bone sarcoma TME**

Dense collagen matrices and aberrant chemokines exclude cytotoxic T cells, while M2 macrophages, MDSCs and Tregs secrete arginase-1, TGF- $\beta$  and adenosine to paralyze effector function (Fig. 2) (13,14). Exhaustion checkpoints, metabolic acidosis and IDO1-driven tryptophan depletion reinforce this immunosuppressive circuit, and immature dendritic cells fail to present antigen, forging an immune-privileged sanctuary that defies therapy (53-56).

**Exclusion and restriction of effector immune cells.** Physical barriers and aberrant chemokine gradients cooperatively limit intratumoral T-cell accumulation (59). The ECM of OS is enriched in collagen I/III, fibronectin and hyaluronan; high tissue stiffness reduces T-cell motility and cytotoxicity *in vitro* and associates with low CD8+ infiltration *in vivo* (60). Chemokine profiling of 22 treatment-naïve OSs revealed a marked paucity of CXCL9/10 and CCL5 concomitant with overexpression of CXCL12 and CCL18, a pattern that

Table I. Bone-related cells in the osteosarcoma tumor microenvironment: Ontogeny, key mediators and immunotherapeutic implications.

First author/s, year	Cell type	Ontogeny in bone	Key immuno-suppressive mediators	Consequences on anti-tumor immunity	Clinically testable intervention	(Refs.)
Canon <i>et al</i> , 2008	Osteoblast-lineage cells	Local mesenchymal stromal cells, RUNX2 <sup>+</sup>	RANKL, Jagged1, IL-6	M2 polarization of TAMs, ↑ PD-L1	Denosumab (RANKL mAb) ↓ M2-TAM 40% <i>in vivo</i>	(42)
Tran <i>et al</i> , 2017	Osteoclasts	Hematopoietic CD11b <sup>+</sup> c-fms <sup>+</sup> precursors	TGF-β (>1 ng ml <sup>-1</sup> ), cathepsin K	Converts CD8 <sup>+</sup> T cells into FOXP3 <sup>+</sup> Tregs; bone destruction releases TGF-β	TGF-β R1 inhibitor galunisertib restores NK cytotoxicity vs. ES	(34)
Zelenay <i>et al</i> , 2015	MSCs	Bone-marrow CCR5 <sup>+</sup> cells recruited via CCL5	PGE2→IDO1 in DCs, COX-2	60% ↓ T-cell proliferation in MLR; MDSC expansion	COX-2 deletion in MSCs improves anti-PD-1 efficacy	(50)
Nicolas-Boluda <i>et al</i> , 2021	Mineralizing osteocytes	Embedded in collagen-hydroxyapatite matrix	YAP/TAZ activation by matrix stiffness (25-35 kPa)	↓ MHC-I, ↑ PD-L1, CTL exclusion	LOXL2 inhibition reduces stiffness and sensitizes to CAR-T	(14)
Dong <i>et al</i> , 2023	Bone-lining endothelial cells	CD31 <sup>+</sup> endothelium-forming type-H vessels	Endothelin-1, CXCL9/10 downregulation under hypoxia	↓ CTL trans-endothelial migration; ↑ PD-L1 on perivascular TAMs	Low-dose metronomic cyclophosphamide normalizes vessels and ↑ CAR-T infiltration	(47)

TAM, tumor-associated macrophage; Treg, regulatory T cell; MLR, mixed lymphocyte reaction; MHC-I, major histocompatibility complex class I; CAR-T, chimeric antigen receptor T cell; YAP/TAZ, Yes-associated protein/transcriptional co-activator with PDZ-binding motif; IL, interleukin; PGE2, prostaglandin E2; IDO1, indoleamine 2,3-dioxygenase 1; COX-2, cyclo-oxygenase-2; LOXL2, lysyl oxidase-like 2; CS, chondrosarcoma; CTL, cytotoxic T lymphocyte.

preferentially recruits CXCR4<sup>+</sup> Tregs and CCR8<sup>+</sup> M2 macrophages while excluding CXCR3<sup>+</sup> CD8<sup>+</sup> T cells (61). Consistently, spatial transcriptomics showed an inverse association between CXCL9/10 levels and distance of CD8<sup>+</sup> T cells from tumor nests (Spearman ρ=-0.63, P<0.01) (62). The clinical implication is that forced intratumoral release of CXCL9 or CXCL10 via oncolytic viruses or STING agonists could enhance ICI efficacy, an approach currently being tested in early-phase trials (NCT05115319).

*Active inhibition of effector cells*

**Immune checkpoint expression.** PD-L1 expression is heterogeneous across bone sarcoma subtypes (63). In OS, 40-60% of primary tumors display ≥1% PD-L1 positivity on malignant cells, yet PD-L1 is more consistently found on TAMs and MDSCs where it associates with M2 polarization markers (CD163 and MRC1) (63). scRNA-seq further resolved two myeloid subsets, FABP5<sup>+</sup> M2 TAMs and IFIT1<sup>+</sup> M1 TAMs, demonstrating that only the former co-express PD-L1 and Galectin-9, thereby mediating T-cell exhaustion through

PD-1 and TIM-3 signaling (64). CTLA-4 is predominantly expressed on infiltrating Tregs rather than on malignant cells; its density is 3.2-fold higher in metastatic lesions compared with primary tumors (65). LAG-3 and TIM-3 co-expression is enriched on CD8<sup>+</sup> T cells in recurrent disease, suggesting that combinatorial blockade (PD-1+LAG-3/TIM-3) may address resistance seen with PD-1 monotherapy (66).

**Treg-mediated suppression.** Tregs constitute 10-25% of CD4<sup>+</sup> tumor-infiltrating lymphocytes (TILs) in OS and exhibit an activated phenotype (FOXP3<sup>high</sup>, CD25<sup>high</sup> and CTLA-4<sup>high</sup>) (67). Functionally, Tregs suppress CD8<sup>+</sup> proliferation *in vitro* via IL-10, TGF-β and IL-35 and physically deplete IL-2 through high-affinity IL-2Rα (68,69). Notably, the Treg/CD8 ratio increases from 0.2 in primary tumors to 0.7 in metastases (P<0.001), paralleling reduced objective response rates to anti-PD-1 therapy in metastatic cohorts (8 vs. 26% in localized disease) (70). Depletion models in murine OS (K7M2) show that transient Treg reduction (anti-CD25) doubles CD8<sup>+</sup> granzyme-B production and restores sensitivity to PD-1 blockade (71).

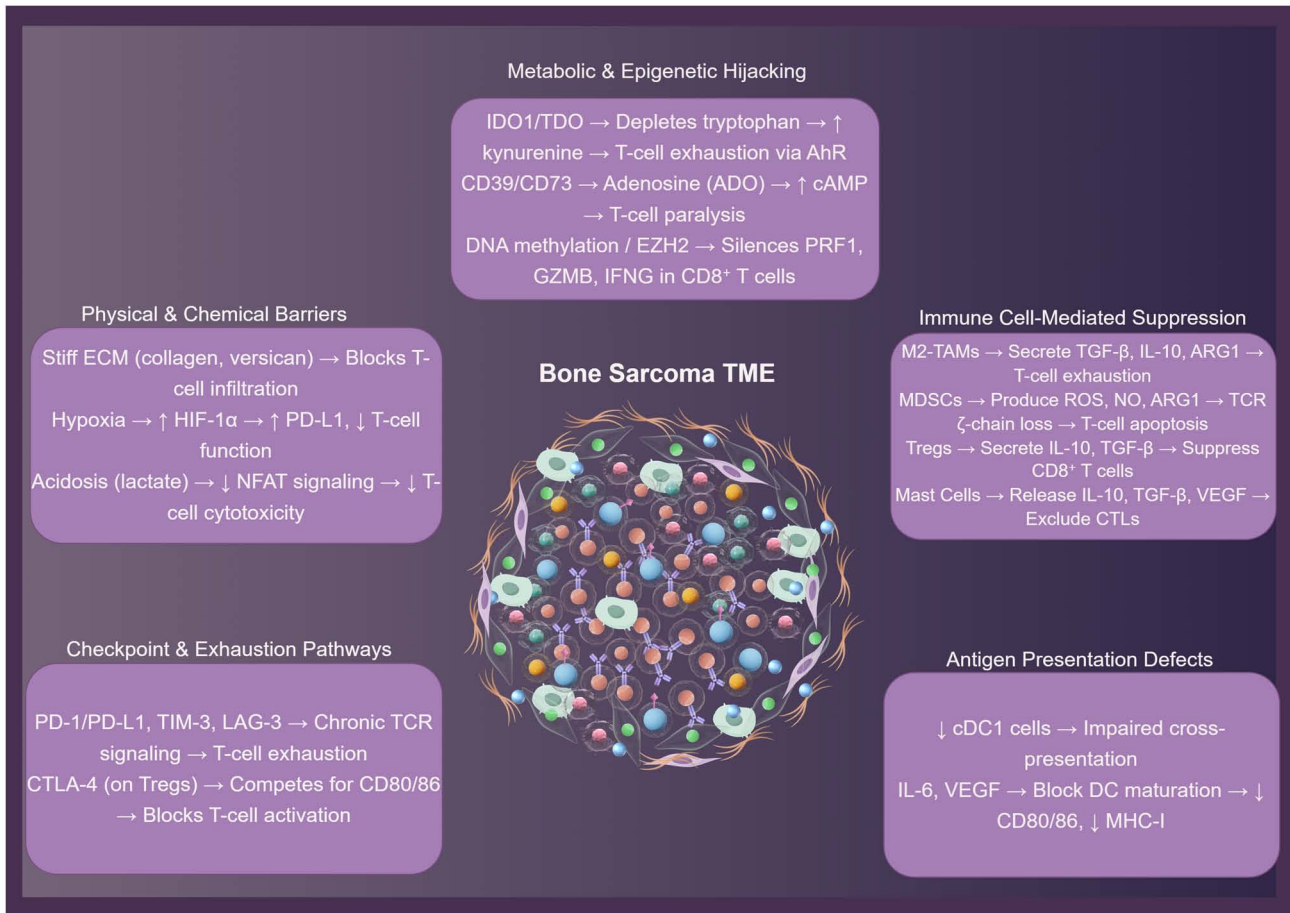


Figure 2. Mechanisms of immunosuppression within the bone sarcoma TME (The figure was created using the online graphic design website Figdraw: [www.figdraw.com](http://www.figdraw.com)). TAM, tumor-associated macrophage; Treg, regulatory T cell; MDSCs, myeloid-derived suppressor cells; CAFs, cancer-associated fibroblasts; ECM, extracellular matrix; PD-L1, programmed death-ligand 1; TIM-3, T-cell immunoglobulin and mucin-domain containing-3; LAG-3, lymphocyte-activation gene 3; IDO1, indoleamine 2,3-dioxygenase 1; ARG1, arginase-1; HIF-1 $\alpha$ , hypoxia-inducible factor-1  $\alpha$ ; ADO, adenosine; KYN, kynurenine; AhR, aryl hydrocarbon receptor; cDC1, conventional type 1 dendritic cell.

**Myeloid cell-mediated suppression.** M2-polarized TAMs (CD68<sup>+</sup>CD163<sup>+</sup>) and G-MDSCs (CD11b<sup>+</sup>CD15<sup>+</sup>) dominate the bone sarcoma TME (72). TAMs secrete arginase-1, which depletes extracellular arginine and arrests T-cell proliferation at the G<sub>0</sub>/G<sub>1</sub> phase (73). *In vitro* co-culture assays demonstrate that arginase inhibition (nor-NOHA) rescues CD8<sup>+</sup> proliferation by 70% (74). MDSCs generate nitric oxide (NO) via iNOS and release ROS; both suppress T-cell receptor (TCR)  $\zeta$ -chain expression levels and promote T-cell apoptosis (75). Pre-clinical models indicate that targeting the colony-stimulating factor 1 receptor (CSF-1R) pathway or pharmacologic iNOS inhibition markedly reduces the density of these suppressive myeloid subsets and enhances immune-checkpoint blockade efficacy, yet prospective clinical validation of their predictive value and safety remains ongoing (76,77).

**Induction of T Cell dysfunction/exhaustion.** Chronic antigen exposure in bone sarcomas drives a progressive exhaustion program (78). sc TCR sequencing revealed oligoclonal expansion (median 47 unique clonotypes per patient) with over-representation of exhausted TCF-1<sup>+</sup>TOX<sup>+</sup> PD-1<sup>high</sup> CD8<sup>+</sup> subsets (79). Continuous PD-1 signaling, reinforced by TIM-3 and LAG-3, upregulates diacylglycerol kinase- $\alpha$ , dampening TCR signaling (80). Metabolic stress further exacerbates

dysfunction: Lactate (15-20 mM) suppresses nuclear factor of activated T-cells (NFAT) nuclear translocation, while adenosine (via CD73/CD39 axis) elevates intracellular cyclic adenosine monophosphate (cAMP), both impairing cytokine production (81). Pre-clinical blockade of the adenosine A2A receptor (A2AR) pathway restores T-cell effector function in hypoxic OS models, providing a rationale for combining adenosine-targeted agents with immune-checkpoint inhibitors in future trials (82).

**Dysfunctional antigen presentation.** Conventional type 1 dendritic cells are scarce (<1% of CD45<sup>+</sup> cells) and display an immature phenotype (CD83<sup>low</sup>CCR7<sup>low</sup>) (83). DC maturation defects are associated with IL-6 and VEGF-A produced by tumor cells, which downregulate co-stimulatory molecules (CD80/86) and impair cross-presentation of tumor antigens (84). Emerging pre-clinical data indicate that intratumoral delivery of a TLR3 agonist can expand cDC1 numbers and amplify CXCL9/10 secretion, thereby enhancing CD8<sup>+</sup> T-cell infiltration; however, formal clinical validation is still pending (85).

**Metabolic competition and immunometabolism.** Metabolic reprogramming within the bone sarcoma TME actively suppresses antitumor immunity (86). Tumor cells exhibit high

Table II. Immune-checkpoint inhibitor trials in bone sarcomas-current evidence.

First author/s, year	Phase	Histology (n)	Regimen	ORR% (n/N)	mPFS/ mOS (mo)	TME-driven resistance mechanism	(Refs.)
Tawbi <i>et al</i> , 2017	II	OS (13) + CS (9)	Pembrolizumab 200 mg q3w	5% (1/22)	2.1 / 11.2	Cold TME (low TIL), genomic quietness, myeloid dominance	(93)
Le Cesne <i>et al</i> , 2019	II	OS (30)	Pembrolizumab ± metronomic cyclophosphamide	0% (0/30)	1.8 / 8.1	Spatial exclusion PD-L1+ cells distant from CTLs	(94)
Davis <i>et al</i> , 2020	I/II	OS (14)	Nivolumab ± ipilimumab q3w	7% (1/14)	2.5 / 14.3	Myeloid-dominant niche; low neoantigen load	(95)
Davis <i>et al</i> , 2022	I/II	OS (14)	Nivolumab + ipilimumab	7% (1/14)	2.6 / 14.8	CXCL12-high stroma excludes CTLs	(96)
Boye <i>et al</i> , 2021	II	OS (28)	Pembrolizumab 200 mg q3w	0% (0/28)	1.9 / 7.5	Mast-cell-TGF-β axis blocks CTL influx	(97)
Palmerini <i>et al</i> , 2025	II	OS (15)	Nivolumab + sunitinib	0% (0/15)	2.2 / 9.0	Hypoxia-driven PD-L1 upregulation; MDSC expansion	(98)
Yang <i>et al</i> , 2024	Trans-lational	OS biopsies	Spatial transcriptomics	Correlative	-	PD-L1+ cells are spatially distant from CD8+ CTLs	(99)
Jiang <i>et al</i> , 2019	Pre-clinical	Murine OS	Anti-PD-1 ± CXCR4 blockade	0 vs. 45% (with CXCR4i)	-	SDF-1/CXCR4 recruits MDSCs that blunt ICI efficacy	(100)

BC, breast cancer; EBC, early breast cancer; HR+, hormone receptor-positive; HER2+, human epidermal growth factor receptor 2-Positive; DFS, disease-free survival; OS, overall survival; IDFS, invasive disease-free survival; pCR, pathological complete response; CTC, circulating tumor cell; RCT, randomized controlled trial; WHI, women's health initiative; DXA, dual-energy X-ray absorptiometry; CRP, C-reactive protein; IL-6, interleukin-6; AI, aromatase inhibitor; SNP, single nucleotide polymorphism; DRFS, distant recurrence-free survival.

glycolytic flux, generating an acidic, lactate-rich milieu that impairs CD8<sup>+</sup> T-cell cytotoxicity and cytokine production, notably via inhibition of NFAT signaling and histone acetylation (87). Concurrently, tumor and stromal cell upregulation of IDO1 depletes tryptophan and produces immunosuppressive kynurenine metabolites, activating the aryl hydrocarbon receptor in T cells and driving exhaustion (88). Furthermore, the CD39/CD73-A2AR adenosine axis is a dominant immunosuppressive pathway; adenosine generated extracellularly suppresses T-cell effector functions via elevated intracellular cAMP. Elevated CD73 expression associates with poor response to PD-1 blockade (88,89). These pathways collectively establish a metabolically hostile environment for effector immune cells.

*Epigenetic modulation of immune cells.* DNA hypermethylation silences perforin 1 (PRF1), granzyme B (GZMB) and IFN $\gamma$  promoters in CD8<sup>+</sup> TILs, whereas H3K27me3 deposition represses T-box transcription factor 21 and eomesodermin loci, locking cells in an exhausted state (90). OS-derived exosomal miR-221-3p downregulates suppressor of cytokine signaling 3 in macrophages, enhancing JAK2-STAT3 signaling and sustaining M2 polarization (91). Conversely, pharmacologic

inhibition of enhancer of zeste homolog 2 (EZH2; tazemetostat) reactivates PRF1 and GZMB transcription in murine models, improving response to PD-1 blockade (92). These data raise the prospect of combining epigenetic modifiers with immune checkpoint inhibitors (ICIs) to overcome adaptive resistance.

**4. Immunotherapy in bone sarcomas: Current landscape and TME-driven challenges**

Building upon the aforementioned mechanistic studies, the clinical record of immune checkpoint and adoptive cell therapies in bone sarcomas is now systematically reviewed. Table II (93-100) summarizes objective response rates from landmark ICI trials, while Table III (35,36,101-124) collates pre-clinical and early-phase adoptive cell therapies (ACT) data, together revealing how the immunosuppressive TME continues to dictate therapeutic outcome.

*ICIs.* The advent of ICIs, particularly targeting the PD-1/PD-L1 and CTLA-4 axes, revolutionized oncology. However, their application in bone sarcomas, primarily OS, has yielded predominantly modest clinical benefits, underscoring the profound influence of the TME in shaping resistance (93,94).

Table III. Adoptive cell therapy in bone sarcomas - pre-clinical and early-phase clinical data.

First author/s, year	Histology (n)	Cell product and target	Study type	ORR/tumor control	Key TME-linked factor/resistance mechanism	(Refs.)
Huang <i>et al.</i> , 2015	E	IGF1R- and ROR1-CAR-T	Pre-clinical	↓ tumor burden	Target expressed but T-cell exhaustion in a hypoxic niche	(104)
Majzner <i>et al.</i> , 2019	OS, ES xenografts	B7-H3-CAR-T (4-1BB $\zeta$ )	Pre-clinical	90% long-term survival	Uniform B7-H3; TAMs exclusion blunted by IL-12-armed CAR-T	(105)
Talbot <i>et al.</i> , 2021	Murine OS (orthotopic)	B7-H3-CAR-T (CD28 $\zeta$ )	Pre-clinical	Marked tumor reduction	Collagen density $\geq 25$ kPa predicts poor CAR-T infiltration	(106)
Zhang <i>et al.</i> , 2022	OS lines and xenografts	B7-H3-CAR-T	Pre-clinical	Complete tumor	ECM stiffness limits T-cell motility	(36)
Cao <i>et al.</i> , 2024	Canine OS (7)	B7-H3-CAR-T + CXCR2	Phase I (canine)	regression 57% ORR (4/7)	CXCL12-rich CAFs stroma reversed by CXCR2 co-expression	(35)
Lake <i>et al.</i> , 2024	OS xenografts	B7-H3-CAR-T + IL-8 homing	Pre-clinical	↑ tumor infiltration and survival	Chemokine-receptor mismatch overcome by IL-8 redirection	(107)
Talbot <i>et al.</i> , 2024	Murine OS	B7-H3-CAR-T CXCR1/2-armed	Pre-clinical	70 vs. 20% control	CXCL9/10 gradient required for optimal trafficking	(108)
Wang <i>et al.</i> , 2019	OS lines and xenografts	CD166/4-1BB CAR-T	Pre-clinical	Tumor growth inhibition	Stromal barrier reduces infiltration	(109)
Charan <i>et al.</i> , 2020	ES metastatic model	GD2-CAR-T + anti-HGF	Pre-clinical	↓ primary and metastatic burden	HGF-rich TME impairs CAR-T; neutralization restores efficacy	(110)
Englisch <i>et al.</i> , 2020	ES xenografts	VEGFR2-CAR-T	Pre-clinical	Tumor growth delay	VEGF-induced suppressive myeloid cells counter CAR-T	(111)
Hsu <i>et al.</i> , 2021	OS/ES lines	EphA2-CAR-T	Pre-clinical	Variable cytotoxicity	Heterogeneous antigen + TGF- $\beta$ -mediated suppression	(112)
Lu <i>et al.</i> , 2019	OS lines	FR $\alpha$ -CAR-T (bispecific adaptor)	Pre-clinical	Target-dependent killing	FR $\alpha$ heterogeneity limits uniform targeting	(113)
Watanabe <i>et al.</i> , 2023	Sarcoma lines	DNAJB8-TCR-T and CAR-T	Pre-clinical	Tumor control <i>in vitro/in vivo</i>	Cancer-stem-cell antigen downregulated under hypoxia	(114)
Mensali <i>et al.</i> , 2023	OS lines and PDX	ALPL-1-CAR-T	Pre-clinical	Marked tumor reduction	ALPL-1 is restricted to the osteoblastic subset; ECM impedes penetration	(115)
Wickman <i>et al.</i> , 2024	OS/ES xenografts	TNC-CAR-T (IL-18R armored)	Pre-clinical	Enhanced survival	IL-18 counters TAM-mediated suppression	(116)
Hu <i>et al.</i> , 2022	OS syngeneic	attIL-12-T cells	Pre-clinical	Eradication of large tumors	Membrane-anchored IL-12 remodels MDSC-rich TME	(117)
Yang <i>et al.</i> , 2022	OS xenografts	attIL-12-PBMC	Pre-clinical	Tumor regression	IL-12 overcomes lactate-induced T-cell paralysis	(118)

Table III. Continued.

First author/s, year	Histology (n)	Cell product and target	Study type	ORR/tumor control	Key TME-linked factor/resistance mechanism	(Refs.)
Hui <i>et al</i> , 2024	OS xenografts	CXCR5 <sup>+</sup> IL-7 <sup>+</sup> CAR-T	Pre-clinical	3-fold ↑ CAR-T persistence	CXCL13 gradient improves T-cell retention	(119)
Adeshakin <i>et al</i> , 2025	OS model	Regnase-1 KO GD2-CAR-T	Pre-clinical	70% tumor control	Regnase-1 deletion creates pro-inflammatory TME	(120)
Hidalgo <i>et al</i> , 2023	OS xenografts	Switchable GD2-CAR-T	Pre-clinical	Tumor regression on-demand	Switch system mitigates fratricide and exhaustion	(121)
Wang <i>et al</i> , 2024	OS model	PET reporter GD2-CAR-T	Pre-clinical	Real-time tracking	Poor persistence linked to hypoxia and nutrient depletion	(122)
Altwater <i>et al</i> , 2021	ES lines	GD2-CAR-T ± HLA-G/E blockade	Pre-clinical	No functional impact	HLA-G/E checkpoint minimally suppresses CAR-T	(123)
Pezzella <i>et al</i> , 2024	Murine OS	GD2-CAR-T ± anti-G-CSF	Pre-clinical	70 vs. 20% control	Tumor-derived G-CSF drives Ly6G <sup>+</sup> MDSC expansion	(124)
Kaczanowska <i>et al</i> , 2024	OS (14) + ES (8)	GD2-CAR-T	Phase I/II	23% ORR (5/22)	High baseline CXCL9/10 and low G-CSF associate with expansion	(125)
Lu <i>et al</i> , 2017	Sarcoma (1/9)	MAGE-A3-TCR-T (HLA-DP)	Phase I/II	100% CR (1/1)	High MAGE-A3 and matched HLA required	(127)
Hamada <i>et al</i> , 2024	Sarcoma lines (OS/ES)	PBF-TCR-T (HLA-A)	Pre-clinical	33% <i>ex vivo</i> response	Antigen loss variants escape detection	(128)

BC, breast cancer; RCT, randomized controlled trial; QoL, quality of life; HR+, hormone receptor-positive; TNBC, triple-negative breast cancer; PFS, progression-free survival; mTOR, mammalian target of rapamycin; AMPK, AMP-activated protein kinase; SCD1, stearoyl-CoA desaturase-1; CRP, C-reactive protein; HOMA-IR, homeostatic model assessment of insulin resistance; IBIS-II, International Breast Cancer Intervention Study II.

**Clinical trial results.** Across the published pembrolizumab, nivolumab and nivolumab-plus-ipilimumab series, objective responses in bone sarcoma rarely exceed single digits. SARC028, the sentinel multicenter phase II trial, enrolled 22 patients with OS or CS and documented only one partial response lasting 32 weeks, yielding an objective response rate of 5% (93). Two confirmatory studies have since reproduced this figure: The PEMBROSARC cohort of 30 heavily pre-treated ( $\geq 2$  prior lines of systemic cytotoxic chemotherapy or targeted therapy) patients with OS had no objective responses at all (94), while the pediatric ADVL1412 expansion treated 14 patients with OS with nivolumab plus ipilimumab and observed just one durable partial response (objective response rate, 7%) (95,96). Single-arm studies using pembrolizumab monotherapy (Boye *et al* (97), 28 patients) or the nivolumab-sunitinib combination [Palmerini *et al* (98); 15 patients] produced identical null response rates.

The mechanistic explanation for this uniformly low activity lies in three interconnected features of the bone-sarcoma TME detailed in ‘Mechanisms of immunosuppression within the bone sarcoma TME’, immunologically ‘cold’ tumors: Spatial mapping shows PD-L1-expressing cells physically separated from CD8<sup>+</sup> CTLs, creating an excluded infiltrate refractory to checkpoint reactivation (99). Genomic quietness: Low mutational burden and minimal neoantigen presentation deprive T cells of the antigenic signal needed for ICI-driven expansion (93). Pronounced myeloid dominance: The SDF-1/CXCR4 axis recruits monocytic MDSCs that outcompete CTLs for glucose and secrete arginase-1, directly neutralizing anti-PD-1 efficacy in pre-clinical models (100). Notably, the lone responder in SARC028 had chondroblastic OS with high PD-L1 expression ( $\geq 50\%$  tumor cells) and brisk peritumoural CD8 infiltration, illustrating that exceptional responders may arise when the tumor deviates from the archetypal ‘cold’ bone-sarcoma microenvironment (93).

**Biomarkers of response/resistance.** PD-L1 expression remains the most interrogated biomarker, yet results are inconsistent. Discordant PD-L1 status between primary and metastatic lesions occurs in 35% of patients with OS, undermining archival tissue reliability (101). In PEMBROSARC, PD-L1 positivity ( $\geq 1\%$ ) was present in 30% of cases but was unassociated with benefit (94). Conversely, Le Cesne *et al* (94) reported that high PD-L1 combined with IDO1 expression enriched for a 10% long-term disease-control subgroup, hinting at combinatorial biomarker utility. Spatial transcriptomics now suggests that the spatial proximity of PD-L1<sup>+</sup> macrophages to CTLs, rather than absolute PD-L1 levels, predicts non-progression (99). Beyond PD-L1, an ‘immune-hot’ signature (CD8<sup>+</sup> CTL/Treg ratio  $> 2$  and low M-MDSC density) emerged as an independent predictor of PFS in the nivolumab-plus-ipilimumab ADVL1412 cohort (HR, 0.31; 95% CI, 0.12-0.78) (96). However, this signature was present in only 6/38 (16%) sarcoma biopsies, underscoring the rarity of immunologically favorable bone sarcomas.

Emerging evidence suggests mast-cell stabilization as a novel resistance mechanism. Mast cells are tissue-resident, c-Kit<sup>+</sup>FcεR1<sup>+</sup> innate immune cells that differentiate in the bone marrow, circulate as progenitors and mature locally under the influence of stem-cell factor, IL-3, IL-33 and CXCL12. In bone sarcomas, mast cells preferentially localize

to the hypoxic tumor margin and along neo-vessels, where they act as central hubs integrating stromal and immune signals (102). Upon activation, mast cells rapidly degranulate histamine, tryptase and chymase, and additionally secrete IL-4, IL-10, VEGF-A, PDGF-B and TGF-β1. These mediators collectively enhance vascular permeability, stimulate CAF proliferation and promote M2-like macrophage polarization, thereby reinforcing an immunosuppressive niche that blunts cytotoxic T-cell influx. Pharmacological stabilization of mast cells with cromolyn or targeted depletion via c-Kit inhibition restores CD8<sup>+</sup> T-cell infiltration and sensitizes OS xenografts to anti-PD-1 therapy, underscoring their therapeutic relevance (44). Mast-cell-derived IL-10 and TGF-β convert macrophages toward M2 and exclude CTLs; pharmacologic stabilization restored PD-L1 blockade sensitivity pre-clinically (44), validation in human studies is required. Finally, host-related factors (human leukocyte antigen loss of heterozygosity, low peripheral blood T-cell clonality) associated with primary resistance in soft-tissue sarcomas warrant investigation in bone sarcomas via ongoing multi-omics studies (such as NCT 04339738) (34,35,103).

In summary, current ICI trials confirm modest single-agent activity in bone sarcomas, driven by an immunologically ‘cold’ and myeloid-dominated TME. Objective responses cluster in rare cases with inflamed, PD-L1-high, CTL-rich tumors, but robust predictive biomarkers are still lacking. Future efforts must integrate spatially resolved TME profiling, systemic immune monitoring and rational combination strategies to overcome primary resistance.

#### ACT

**CAR T-Cells: Preclinical/clinical progress.** CAR T cells therapy has shown notable preclinical potential in bone sarcomas, targeting various tumor-associated antigens. Early work demonstrated the efficacy of IGF1R- and ROR1-specific CAR T cells against sarcoma cell lines and xenografts, highlighting IGF1R as a particularly potent target (104). Subsequent research identified B7-H3 (CD276) as a highly expressed pan-cancer antigen in pediatric solid tumors, including OS and ES. B7-H3-CAR T cells exhibited robust antitumor activity in multiple preclinical OS models, markedly reducing tumor burden and improving survival (36,105,106). This efficacy was further enhanced by strategies to overcome TME-driven homing limitations. Engineering B7-H3-CAR T cells to express chemokine receptors such as CXCR2 or CXCR1/CXCR2 ligands (for example, IL-8) or redirecting them towards chemokines (CXCL9 and CXCL10) abundant in OS models, considerably improved tumor infiltration and antitumor potency compared with standard CAR T cells (35,107,108). Similarly, CAR T cells targeting CD166/4-1BB showed efficacy against OS *in vitro* and *in vivo*, inducing cytotoxicity and inhibiting tumor growth (109). Other promising preclinical targets include GD2 in ES [where combining GD2-CAR T cells with hepatocyte growth factor-neutralizing antibody prevented metastasis (110)], VEGFR2 in ES vasculature (111), EphA2 [though efficacy was variable (112)], folate receptor  $\alpha$  (FR $\alpha$ ) via a bispecific adaptor approach (113), cancer stem cell antigens DnaJ Heat Shock Protein Family Member B8 (DNAJB8) (114) and alkaline phosphatase, biomineralization associated-1 (115) and oncofetal tenascin C

using IL-18R-supported CARs (116). Membrane-anchored, tumor-targeted IL-12 expressed on CAR T cells or PBMCs also demonstrated potent antitumor activity against heterogeneous OS models by remodeling the TME (117,118). Recent strategies involve enhancing homing via CXCR5/IL-7 co-expression (119), targeting immunosuppressive pathways such as Regnase-1 to create a proinflammatory TME (120) or utilizing switchable CAR systems for improved safety (121).

Despite promising preclinical results, translating CAR T-cells efficacy to the clinic for solid tumors such as bone sarcomas faces major hurdles imposed by the TME. Trafficking to tumor sites remains a key barrier. Poor homing has been observed, partly due to inadequate chemokine receptor expression on CAR T cells mismatched with the chemokine profile of the TME (108,111). Persistence of functional CAR T cells *in vivo* is often limited. Wang *et al* (122) demonstrated the utility of PET reporter gene imaging to monitor CAR T cells location and persistence, revealing challenges in maintaining therapeutic cell numbers within solid tumors. Factors contributing to poor persistence include T-cell exhaustion within the immunosuppressive TME and potential fratricide when targeting widely expressed antigens. Suppression by the TME is a dominant challenge. The TME fosters immunosuppressive cell populations (TAMs, MDSCs and Tregs) and expresses immune checkpoint molecules. While Altvater *et al* (123) found that HLA-G and HLA-E, though expressed in ES, had limited functional impact on GD2-CAR T cells *in vitro*, other immunosuppressive mechanisms are potent. Tumor-derived soluble factors, particularly granulocyte colony-stimulating factor, have been shown to create an immunosuppressive myeloid-rich TME that markedly impairs the efficacy of GD2-CAR T cells in OS models (124). The physical barriers of the tumor stroma and hypoxia further impede CAR T cell function. Clinical experience with CAR T cells in bone sarcomas remains limited primarily to early-phase trials, often showing modest activity compared with hematologic malignancies. Recent analyses, such as the identification of immune determinants of CAR T cell expansion in GD2-CAR T treated patients with solid tumor (including OS/ES), underscore the complex interplay between patient factors, product attributes and the TME that dictates clinical outcomes (125). Kaczanowska *et al* (125) found that early expansion kinetics and T cell phenotypes notably influenced outcomes in GD2-CAR trials for sarcomas and neuroblastoma, while Arnett and Heczey (126) emphasized that beyond T cell fitness, the immunosuppressive TME is a major limiting factor requiring combination approaches.

**TCR-Engineered T Cells.** T cell receptor-engineered T (TCR-T) cell therapy and TIL therapy represent alternative ACT strategies, but their application in bone sarcomas is less advanced than CAR T therapy and faces distinct challenges. TCR-T cells can target intracellular antigens presented by MHC molecules, potentially broadening the targetable antigen repertoire. Lu *et al* reported a clinical trial using an MHC class II-restricted TCR targeting the cancer germline antigen MAGE-A3. While the trial included patients with various types of metastatic cancer, one patient with metastatic sarcoma (unspecified subtype) achieved a complete response lasting >24 months, demonstrating the potential therapeutic activity of TCR-T cells in sarcoma (127). Recently, Hamada *et al* (128)

developed TCR-T cells targeting the sarcoma-associated antigen papillomavirus binding factor (PBF). These TCR-T cells demonstrated specific cytotoxicity against PBF-positive sarcoma cell lines *in vitro* and inhibited tumor growth in xenograft models. Watanabe *et al* (114) targeted the cancer stem cell antigen DNAJB8 with TCR-T cells, showing efficacy against various solid tumors *in vitro* and *in vivo*, though specific bone sarcoma data were limited.

TCR-T therapy faces considerable hurdles in bone sarcomas. Key challenges include identifying truly tumor-specific intracellular antigens shared across subtypes, dependence on tumor MHC expression, intratumoral heterogeneity enabling escape and the critical risk of off-target toxicity due to TCR cross-reactivity (114,128). Furthermore, as with CAR T cells, TCR-T cells must overcome the profoundly immunosuppressive TME to traffic, persist and function effectively, with specific bone sarcoma TME interaction data currently limited.

**Oncolytic viruses, cancer vaccines.** Pre-clinical studies show that oncolytic viruses can control OS growth, yet the immunocompetent microenvironment rapidly blunts efficacy (129-131). Intratumoral Semliki Forest virus encoding HSV-TK shrank orthotopic 143B-luc tumors by 74% in nude mice, but complete regressions were absent and viral genomes disappeared within 7 days, leaving the contribution of antitumor immunity unaddressed (129). Similarly, intravenous reovirus cleared Ras-activated xenografts yet failed against A673 or SJS-A-1 lesions, and its benefit was lost in syngeneic K7M2 mice owing to neutralizing antibodies and T-cell-mediated viral clearance (130).

Systemic delivery is further complicated by metastatic burden. Christie *et al* (131) delivered mLIGHT-armed myxoma virus intravenously to syngeneic 66.1 lung-metastatic OS; median survival doubled when nodule counts were <100, but mice with >200 lesions showed rapid rebound growth driven by hypoxia-associated PD-L1 upregulation. These data indicate that high antigen load and immune suppression within the bone sarcoma TME impose a clear therapeutic ceiling.

Large-animal studies corroborate these limitations. Laborda *et al* (132) treated seven spontaneous canine OSs with intratumoral ICOVIR-16K; two dogs achieved partial metabolic responses and one complete pathological response, yet neutralizing antibody titres >1:1,000 were detected after the second dose, coinciding with viral clearance in serial biopsies. The findings underscore the challenge of maintaining viral replication in immunocompetent, outbred hosts and reinforce the need for transient B-cell depletion or alternative dosing schedules.

Live-attenuated *Listeria monocytogenes* vaccines offer a complementary strategy. Musser *et al* (133) administered Lm-LLO-E7 to 15 OS-bearing dogs; although only mild pyrexia and lymphopenia occurred, median survival appeared prolonged vs. historical controls (234 vs. 180 days). However, lack of randomization and heterogeneous adjuvant chemotherapy preclude definitive efficacy claims and anti-*Listeria* immunity may limit booster efficacy.

Finally, antigen heterogeneity threatens peptide-based vaccination. Chen *et al* (134) screened 87 treatment-naïve OSs; melanoma-associated antigen A4, New York esophageal squamous cell carcinoma-1 and preferentially expressed antigen in melanoma were expressed in 28, 20 and 15% of

tumors respectively, with only 6% co-expressing  $\geq 2$  antigens. Taken together, these studies highlight the dual hurdles of TME-mediated immune suppression and tumor-intrinsic antigen diversity; rational combinations of oncolytic viruses or vaccines with checkpoint blockade, radiotherapy and personalized neoantigen libraries are required to unlock their clinical potential.

## 5. Therapeutic targeting of the bone sarcoma TME

Pre-clinical reprogramming strategies, CSF-1R inhibition, LOXL2 knockdown, hypoxia-activated prodrugs and EZH2 blockade, restore CTL infiltration and sensitize tumors to checkpoint blockade (Table IV) (55,61,135-144). Composite biomarker panels integrating stiffness, hypoxia scores and immune infiltrate predict 2-3-fold increases in durable regressions across OS models.

*Reprogramming immunosuppressive myeloid cells.* High-dimensional analyses concur OS is dominated by arginase-1<sup>+</sup> M2-TAMs and Ly6G<sup>+</sup> monocytic MDSCs (61,145). VEGF-A and P2RX7 signaling fuel tumor growth and instruct M2 polarization via PI3K/Akt/mTOR (135,136). Silencing VEGF-A (135) or inhibiting P2RX7 (136) reduced tumor growth and CD163<sup>+</sup> macrophages by 50% in OS models. However, in ES, targeting extracellular vesicles restored DC maturation only without TGF- $\beta$ , indicating context-dependent myeloid reprogramming signals (146). These convergent yet conditional data argue that multi-pathway blockade is required for durable reprogramming.

*Translation strategies:* Systemic CSF-1R inhibition (pexidartinib) eradicated >70% M2-TAMs in mice, tripled CD8<sup>+</sup> TILs, but caused grade-3 hepatotoxicity in 25% of pediatric patients with only transient responses (145). While promising, repeated intralesional injection is impractical for multifocal disease, and long-term immunogenicity is unknown.

*Modulating the ECM and CAFs barrier.* Collagen cross-linking enzyme LOXL2 is a central regulator of ECM stiffness in OS. LOXL2 knockdown reduced stiffness (35 to 15 kPa), doubled doxorubicin penetration and improved CAR-T infiltration (145). Paradoxically, partial ECM degradation increased metastasis by releasing VEGF-sequestered matrices (138), suggesting indiscriminate collagenolysis is counterproductive. This underscores the need for spatiotemporally controlled strategies, such as photo-activatable MMP-9 inhibitors.

CAFs fortify barriers via paracrine TGF- $\beta$  and CXCL12. CLTC-TFG signaling in CAFs upregulates TGF- $\beta$ , excluding CD8<sup>+</sup> T cells (139). The bifunctional anti-PD-L1/TGF- $\beta$  antibody TQB2858 achieved a 33% objective response rate in relapsed OS (140), yet CAFs heterogeneity predicted variable CXCL12 levels and inconsistent T-cell recruitment. To address plasticity, membrane-anchored IL-12 T cells converted FAP<sup>+</sup> CAFs to an inflammatory phenotype, reduced collagen by 60% and improved CAR-T persistence (141). Unfortunately, sustained IL-12 induced cachexia in 20% of mice, necessitating inducible expression systems.

*Vascular normalization and hypoxia alleviation.* VEGF-A overexpression drives chaotic vasculature (135,142). Anti-VEGF

therapy normalizes vessels preclinically, but clinical bevacizumab monotherapy yielded only 18% 6-month PFS. Mechanistically, it exacerbated hypoxia, upregulated HIF-1 $\alpha$ , PD-L1 and expanded MDSCs (145). Conversely, low-dose metronomic cyclophosphamide increased pericyte coverage and doubled CAR T cells infiltration without worsening hypoxia, illustrating the importance of dose scheduling.

Hypoxia-activated prodrugs such as TH-302 kill hypoxic cells. Combined with anti-PD-1, it improved survival in metastatic OS mice (55). However, variable hypoxic thresholds and a lack of consensus imaging biomarkers hinder application. Integrating <sup>18</sup>F-MISO PET with circulating hypoxia gene signatures may stratify responders, but needs validation.

*Metabolic reprogramming: IDO, lactate and adenosine pathways.* IDO1 is upregulated in 60% of OS and associated with kynurenine-mediated T-cell suppression (143). Epacadostat plus pembrolizumab produced a 33% ORR, yet IDO1 expression did not predict benefit, possibly due to compensatory tryptophan 2,3-dioxygenase activation (145). Dual IDO/TDO inhibitors are under investigation, with off-target hepatic toxicity a concern.

Elevated lactate suppresses NFAT signaling and granzyme-B transcription (147,148). Monocarboxylate transporter 1/4 blockade restored CD8<sup>+</sup> function *ex vivo*, but caused rebound glycolysis and hyperlactatemia in mice (147). Adenosine pathway blockade enhanced GD2-CAR-T expansion and yielded partial responses in 2/6 canine patients with OS (145); however, variable CD73 expression (>45% across biopsies) emphasizes the need for companion diagnostics.

*Epigenetic modulators of immune function.* EZH2 overexpression silences MHC-I and T-cell chemokine genes (144). EZH2 inhibitor tazemetostat restored HLA-A/B/C expression and improved CAR-T recognition; combined with anti-PD-1, eradicated tumors in 60% of mice (144). Continuous dosing raised stem-cell toxicity concerns, necessitating intermittent delivery. Histone deacetylase (HDAC) inhibition (entinostat) increased CXCL9/10 and reduced Tregs, but caused dose-limiting thrombocytopenia. DNA methyltransferase (DNMT) inhibitor decitabine demethylated IFNG/GZMB promoters in exhausted TILs, yet myelosuppression halted dose escalation (145). Collectively, epigenetic therapy is a promising immune-sensitizing adjunct, but optimal scheduling and predictive biomarkers remain undefined.

## 6. Preclinical models and emerging technologies

Translating the aforementioned mechanistic insights and combination strategies into reliable clinical benefit demands experimental platforms that faithfully replicate the mineralized, immune-privileged bone sarcoma niche. Integrating stiffness-tunable 3D hydrogels with humanized mouse models now enables longitudinal tracking of CAR T cells trafficking, myeloid reprogramming and ECM modulation, thereby accelerating the validation of biomarker-driven regimens before paediatric trial entry.

*Limitations of conventional models.* Conventional preclinical models, including cell monolayers and immunodeficient

Table IV. Therapeutic strategies targeting the bone sarcoma TME.

First Author/s, year	Therapy (agent / modality)	TME axis modulated	Key reported outcome(s)	Validated biomarker/ resistance cue	Sarcoma model(s)	(Refs.)
Liu <i>et al.</i> , 2023	Single-cell TME mapping + CSF-IR inhibitor (Pexidartinib)	Reprogram M2-TAMs → M1	↓ CD163 <sup>+</sup> macrophages 70%; tripled granzyme-B <sup>+</sup> CD8 <sup>+</sup> TILs; 70% tumor regression	Hepatotoxicity; requires dose optimization	Orthotopic 143B OS; canine spontaneous OS	(61)
Gu <i>et al.</i> , 2019	Dual-shRNA VEGF-A knockdown	Angiogenesis + M2-TAM reprogramming	50% ↓ tumor growth; 50% ↓ CD163 <sup>+</sup> TAMs	PI3K/Akt/mTOR dependency; TGF-β context-dependency	143B OS xenograft	(135)
Zhang <i>et al.</i> , 2019	P2RX7 antagonist	VEGF-P2RX7-M2 axis	↓ p-Akt; ↓ CD163 <sup>+</sup> TAMs; ↓ tumor burden	TGF-β co-blockade required for full effect	HOS/MNNG OS	(136)
Dong <i>et al.</i> , 2024	ZIF-8-encapsulated Pexidartinib delivered by M1 macrophages	M2-TAM depletion without systemic toxicity	70% tumor regression; no liver injury	Repeated intra-lesional injection needed; NP immunogenicity unknown	Orthotopic 143B OS	(137)
Gutiérrez <i>et al.</i> , 2021	LOXL2 CRISPR knockdown	ECM stiffness/collagen cross-linking	Young's modulus 35 → 15 kPa; doubled doxorubicin penetration; ↑ CAR-T infiltration	Partial degradation ↑ VEGF release and metastasis risk	OS xenografts	(138)
Shijie <i>et al.</i> , 2021	CLTC-TFG axis inhibitor	CAFs-derived TGF-β secretion	30% tumor growth inhibition; ↑ CD8 <sup>+</sup> TILs	CAFs heterogeneity → variable TGF-β expression	OS cell lines and xenografts	(139)
Xie <i>et al.</i> , 2023	Bifunctional anti-PD-L1/ TGF-β antibody TQB2858	CAFs-derived TGF-β blockade	33% ORR in relapsed OS; CXCL12 predicts T-cell recruitment	CXCL12-high stroma resistance	Human OS (phase Ib)	(140)
Hu <i>et al.</i> , 2024	Membrane-anchored IL-12 T cells (attIL-12-T)	CAFs reprogramming and ECM degradation	60% ↓ collagen; 3-fold ↑ CAR-T persistence	IL-12-induced cachexia (20% mice); switchable systems needed	OS PDX	(141)
Kong <i>et al.</i> , 2019	Low-dose metronomic cyclophosphamide	Vessel normalization	↑ Pericyte coverage; doubled CAR-T infiltration; no ↑ hypoxia	Schedule-dependent balance	Murine ES	(142)
Zhao <i>et al.</i> , 2023	Hypoxia-activated prodrug TH-302 + anti-PD-1	Hypoxia alleviation and ICI synergy	Median survival 28 → 52 days; 50% ↓ lung mets	Variable hypoxic thresholds; imaging biomarker pending	Metastatic 143B OS	(55)
Li <i>et al.</i> , 2023	IDO1 inhibitor Epacodostat + pembrolizumab	Tryptophan-kynurenine axis	33% ORR in heavily pre-treated pts	Compensatory TDO activation; IDO1 IHC not predictive	Human OS (phase Ib)	(143)
Shan <i>et al.</i> , 2025	EZH2 inhibitor Tazemetostat + anti-PD-1	Epigenetic re-activation of MHC-I and chemokines	Tumor eradication in 60% mice; restored HLA-A/B/C	Continuous dosing → stem-cell toxicity; intermittent NP delivery under study	OS syngeneic model	(144)

TME, tumor microenvironment; TAM, tumor-associated macrophage; MDSC, myeloid-derived suppressor cell; ECM, extracellular matrix; CAR-T, chimeric antigen receptor T-cell; IDO1, indoleamine-2,3-dioxygenase 1; PD-L1, programmed death-ligand 1; TGF-β, Transforming Growth Factor-β; CSF1R, colony-stimulating factor 1 receptor; EZH2, enhancer of zeste homolog 2; VEGF, vascular endothelial growth factor; HIF-1α, hypoxia-inducible factor-1 α; A2AR, adenosine A2A receptor.

xenografts, inadequately recapitulate the spatial, mechanical and immunosuppressive features of bone sarcoma TME. *In vitro* 2D cultures fail to model mineralized bone matrices, which physically impede CAR-T cell trafficking and alter metabolic crosstalk between tumor cells and stromal components such as osteoblasts or marrow adipocytes (149,150). Murine xenograft models (such as NOD-SCID) lack functional human immune systems, rendering them incapable of evaluating immunotherapies dependent on human-specific antigen presentation or checkpoint interactions. For instance, such models could not predict the clinical failure of HER2-targeted CAR T cells in OS, which later was attributed to TME-driven exhaustion markers (PD-1, TIM-3) and TGF- $\beta$ -mediated suppression (149,151). Even syngeneic mouse models exhibit interspecies discrepancies in cytokine networks; the TGF- $\beta$ /osteopontin (OPN) axis is key for osteoclast-mediated immunosuppression in human bone metastases, poorly mirrored in murine systems, leading to overstated efficacy of immune checkpoint blockade in bone tumors (152). These limitations underscore a key gap: Conventional models cannot simulate the dynamic immunosuppressive reprogramming induced by bone-specific niches, resulting in unreliable therapeutic predictions.

*Advanced immunocompetent and humanized platforms.* To address these shortcomings, genetically engineered and humanized murine platforms incorporating functional human immunity have emerged (153,154). huHSC-NOG mice reconstituted with human hematopoietic stem cells enable long-term ( $\geq 6$  months) study of human T-cell differentiation and memory responses, making them ideal for evaluating sustained immunotherapy efficacy (153). For example, F. Hoffmann-La Roche Ltd's CEA-TCB bispecific antibody combined with atezolizumab (anti-PD-L1) showed synergistic tumor reduction in huHSC-NOG models of colorectal cancer, a finding later validated clinically (155,156). Conversely, huPBMC-NOG models, which rapidly reconstitute mature T cells within 2-4 weeks, are suited for short-term assessments of T-cell-engaging therapies such as blinatumomab (157). However, their utility is constrained by graft-vs.-host disease) and deficient B-cell reconstitution, limiting studies on antibody-dependent cellular cytotoxicity (158).

Advanced 3D engineered systems now integrate biomechanical cues to mimic bone TME pathophysiology. Stiffness-tunable hydrogels (such as poly-aspartate scaffolds) revealed that matrix rigidity  $>40$  kPa, mimicking mineralized bone, induces YAP overexpression in OS cells, synergizing with TNF- $\alpha$  from TAMs to drive STAT3-mediated chemoresistance (159). These platforms also demonstrate context-dependent therapeutic vulnerabilities; STAT3 inhibition reversed doxorubicin resistance in stiff 3D models but showed minimal efficacy in 2D cultures (151). For giant cell tumor of bone (GCTB), mass cytometry of patient-derived samples identified denosumab-induced depletion of  $\gamma\delta$ TCR+ osteoclast-like giant cells and expansion of cytotoxic CD8+ T cells, a shift not reproducible in non-humanized models (160). Despite progress, discrepancies persist: while 3D models predict enhanced CAR-T cytotoxicity under dynamic flow, clinical translation remains hampered by poor infiltration into osteoid-rich niches 5.

*sc, spatial and high-dimensional technologies.* sc and spatial omics technologies are dissecting the cellular heterogeneity and topographical drivers of immunotherapy resistance in bone sarcomas. Mass cytometry (CyTOF) of GCTB identified a spatially restricted PD-1hiTIM-3+CD69+ CD8+ T-cell population juxtaposed with SIRP $\alpha$ + TAMs, suggesting localized exhaustion within the TME (161). In OS, multi-omics integration of transcriptomic and sc data defined a palmitoylation-driven metabolic-immune subtype characterized by ZDHHC3/21/23 upregulation, which induces 'cold tumor' phenotypes via dual suppression of MAPK signaling and CD8+ T-cell infiltration. High-risk patients, as defined by a palmitoylation-driven prognostic score (PPS) above the 75th percentile, showed resistance to PD-L1 inhibitors in the IMvigor210 cohort, highlighting this subtype's clinical relevance (162).

Spatial transcriptomics further maps cytokine gradients underpinning immunosuppressive niches. In bone metastases, osteoclast-derived OPN creates CXCL12-rich ecological niches that sequester Tregs and exclude cytotoxic T cells, a mechanism validated through *in situ* hybridization in clinical biopsies (152). Radiation modeling in microphysiological systems revealed that proton therapy amplifies localized TGF- $\beta$  secretion from damaged osteoblasts, spatially associating with PD-L1 upregulation in surviving tumor cells (159). However, technological constraints remain: Current spatial methods lack resolution for bone's mineralized matrix and sc datasets are biased toward non-mineralized zones due to tissue dissociation artifacts (163). Discrepancies also arise in immune subset classification; CyTOF-defined TAM subsets in GCTB contradict scRNA-seq annotations due to antibody specificity issues vs. dropout effects in sequencing (164,165).

## 7. Future directions and translational challenges

The next translational leap hinges on replacing PD-L1-centric paradigms with multidimensional TME biomarkers, refining patient stratification through dynamic profiling and engineering bone-selective delivery systems that respect skeletal physiology. Integrating TME modulators demands rigorous longitudinal toxicity surveillance, especially in pediatric populations. Collaborative, biomarker-driven trials embedding real-time immune-monitoring and skeletal health endpoints are indispensable to convert mechanistic insights into durable clinical benefit. Multiplex IHC and spatial transcriptomics of OS biopsies reveal CD8+ T cells proximal to antigen-presenting fibroblasts predict prolonged metastasis-free survival, while high neutrophil-to-CD8+ distance associates with pembrolizumab resistance (166). scRNA-seq resolved a metabolically distinct arginine-depleting TAM cluster inversely associating with post-chemotherapy T-cell expansion (167). However, CyTOF antibody cross-reactivity in mineralized tissue overestimates TAM frequency by  $\sim 30\%$  vs. transcriptomics, highlighting the need for orthogonal validation (20). Composite signatures integrating spatial proximity, metabolic flux and cross-platform profiling likely outperform PD-L1 alone, but standardization remains a challenge.

Unsupervised clustering of 84 OS transcriptomes identified three TME subtypes: 'immune-hot' (CXCL9/PD-L1<sup>high</sup>),

‘myeloid-rich/cold’ (CSF1R/STAT3<sup>high</sup>) and ‘fibrotic-desert’ (COL1A1<sup>high</sup>/CD45<sup>low</sup>) (168). In SARC028, pembrolizumab response was confined to immune-hot tumors (objective response rate, 38%), while myeloid-rich tumors progressed rapidly despite PD-L1 (169). Conversely, neoadjuvant axitinib plus pembrolizumab converted 5/9 myeloid-rich tumors to immune-active and tripled CD8<sup>+</sup> density, achieving 66% 3-month PFS (170). These findings illustrate dynamic conversion is achievable, but baseline stratification is insufficient; longitudinal TME monitoring is required to guide adaptive combinations.

The mineralized matrix and high interstitial pressure limit penetration of antibodies and cellular therapeutics (171). Osteotropic peptide (Asp-Ser-Ser)-modified liposomal alendronate achieved 7-fold higher OS accumulation and reduced tumor burden when loaded with doxorubicin (172). Anti-CD117-conjugated mesoporous silica nanoparticles co-delivering imatinib and STAT3 siRNA deplete MDSCs and sensitize to PD-1 blockade (173). Heterogeneity in pediatric vs. adult bone density may impede nanoparticle extravasation (174), necessitating patient-specific models calibrated with PET perfusion data.

Chronic CSF1R inhibition in adolescent mice transiently decreased trabecular bone volume (BV/TV-22%) due to impaired osteoclastogenesis (175). Combined with PD-1 blockade, sustained Treg reduction led to persistent IFN- $\gamma$  elevation and prolonged suppression of bone formation markers (osteocalcin -35% at 12 weeks), raising fracture risk concerns in growing patients (176). Conversely, local low-dose irradiation (8Gy) followed by GD2-CAR-T infusion increased bone mineral density at metastatic sites via T-cell-mediated osteoblast activation (177). These divergent outcomes underscore the necessity of integrating serial skeletal imaging and biomechanical testing into TME-targeting trials.

Pre-operative DNMT inhibitor (5-azacytidine) plus HDAC inhibitor (entinostat) upregulated neoantigens and synergized with doxorubicin, reducing lung micrometastases by 90% in mice (178). Followed by GD2-CAR-T, the triple combination extended median survival to 85 vs. 42 days for chemo alone (179). However, a phase I study combining pembrolizumab with standard MAP reported unexpected early cardiotoxicity, possibly due to PD-1 blockade enhancing doxorubicin-induced oxidative stress (180). Rational sequencing and dose de-escalation informed by real-time TME profiling are key to maximize synergy while limiting toxicities.

Despite compelling pre-clinical data, only two registered trials (NCT04443235 and NCT05121269) prospectively stratify patients with bone sarcoma by integrated TME signatures. Early results from NCT04443235, a phase II study allocating immune-hot OS to pembrolizumab plus stereotactic radiotherapy and myeloid-rich tumors to CSF1R inhibitor pexidartinib plus pembrolizumab, show an interim overall response rate of 45 vs. 11% in historical controls. Cross-trial comparison reveals that trials lacking biomarker selection consistently report objective response rate below 15%, reinforcing the key impact of patient enrichment. Standardized tissue acquisition protocols, centralized multiplex imaging pipelines and open-access data repositories are proposed to accelerate validation of next-generation biomarkers and ensure reproducibility across centers.

## 8. Conclusion

Current regimens leave metastatic bone sarcomas largely incurable because the immunosuppressive, mineralized and metabolically hostile TME repels effector immunity. Integrating sc, spatial and functional data across OS, ES and CS reveals subtype-specific immune archetypes, tractable stromal targets and delivery barriers. Translation now demands biomarker-driven, bone-selective combinations with real-time monitoring to convert mechanistic insight into durable cures.

## Acknowledgements

Not applicable

## Funding

No funding was received.

## Availability of data and materials

Not applicable.

## Authors' contributions

WL contributed to conceptualization, literature review, writing (original draft) and visualization. LL contributed to literature review, writing (original draft) and retrieve literature. YJ contributed to writing (review and editing) and resources. XY contributed to supervision, project administration, writing (review and editing, and funding acquisition). All authors have read and approved the final manuscript. Data authentication not applicable.

## Ethics approval and consent to participate

Not applicable.

## Patient consent for publication

Not applicable.

## Competing interests

The authors declare that they have no competing interests.

## References

1. Strauss SJ, Frezza AM, Abecassis N, Bajpai J, Bauer S, Biagini R, Bielack S, Blay JY, Bolle S, Bonvalot I, *et al*: Bone sarcomas: ESMO-EURACAN-GENTURIS-ERN PaedCan clinical practice guideline for diagnosis, treatment and follow-up. *Ann Oncol* 32: 1520-1536, 2021.
2. Bray F, Laversanne M, Sung H, Ferlay J, Siegel RL, Soerjomataram I and Jemal A: Global cancer statistics 2022: GLOBOCAN estimates of incidence and mortality worldwide for 36 cancers in 185 countries. *CA Cancer J Clin* 74: 229-263, 2024.
3. Perry JA, Kiezun A, Tonzi P, Van Allen EM, Carter SL, Baca SC, Cowley GS, Bhatt AS, Rheinbay E, Peadarallu CS, *et al*: Complementary genomic approaches highlight the PI3K/mTOR pathway as a common vulnerability in osteosarcoma. *Proc Natl Acad Sci USA* 111: E5564-E5573, 2014.

4. Behjati S, Tarpey PS, Sheldon H, Martincorena I, Van Loo P, Gundem G, Wedge DC, Ramakrishna M, Cooke SL, Pillay N, *et al*: Recurrent PTPRB and PLCG1 mutations in angiosarcoma. *Nat Genet* 46: 376-379, 2014.
5. Marina NM, Smeland S, Bielack SS, Bernstein M, Jovic G, Krailo MD, Hook JM, Arndt C, van den Berg H, Brennan B, *et al*: Comparison of MAPIE versus MAP in patients with a poor response to preoperative chemotherapy for newly diagnosed high-grade osteosarcoma (EURAMOS-1): An open-label, international, randomised controlled trial. *Lancet Oncol* 17: 1396-1408, 2016.
6. Gaspar N, Hawkins DS, Dirksen U, Lewis IJ, Ferrari S, Le Deley MC, Kovar H, Grimer R, Whelan J, Claude L, *et al*: Ewing sarcoma: Current management and future approaches through collaboration. *J Clin Oncol* 33: 3036-3046, 2015.
7. van Maldegem AM, Gelderblom H, Palmerini E, Dijkstra SD, Gambarotti M, Ruggieri P, Nout RA, van de Sande MA, Ferrari C, Ferrari S, *et al*: Outcome of advanced, unresectable conventional central chondrosarcoma. *Cancer* 120: 3159-3164, 2014.
8. Nakano K: Challenges of systemic therapy investigations for bone sarcomas. *Int J Mol Sci* 23: 3540, 2022.
9. Tlemsani C, Larousserie F, De Percin S, Audard V, Hadjadj D, Chen J, Biau D, Anract P, Terris B, Goldwasser F, *et al*: Biology and management of high-grade chondrosarcoma: An Update on targets and treatment options. *Int J Mol Sci* 24: 1361, 2023.
10. Yuan Z, Li Y, Zhang S, Wang X, Dou H, Yu X, Zhang Z, Yang S and Xiao M: Extracellular matrix remodeling in tumor progression and immune escape: From mechanisms to treatments. *Mol Cancer* 22: 48, 2023.
11. Naser R, Fakhoury I, El-Fouani A, Abi-Habib R and El-Sibai M: Role of the tumor microenvironment in cancer hallmarks and targeted therapy (Review). *Int J Oncol* 62: 23, 2023.
12. Alfranca A, Martinez-Cruzado L, Tornin J, Abarrategi A, Amaral T, de Alava E, Menendez P, Garcia-Castro J and Rodriguez R: Bone microenvironment signals in osteosarcoma development. *Cell Mol Life Sci* 72: 3097-3113, 2015.
13. Zhou Y, Yang D, Yang Q, Lv X, Huang W, Zhou Z, Wang Y, Zhang Z, Yuan T, Ding X, *et al*: Single-cell RNA landscape of intratumoral heterogeneity and immunosuppressive microenvironment in advanced osteosarcoma. *Nat Commun* 11: 6322, 2020.
14. Nicolas-Boluda A, Vaquero J, Vimeux L, Guilbert T, Barrin S, Kantari-Mimoun C, Ponzio M, Renault G, Deptula P, Pogoda K, *et al*: Tumor stiffening reversion through collagen crosslinking inhibition improves T cell migration and anti-PD-1 treatment. *Elife* 10: e58688, 2021.
15. Shurin MR and Umansky V: Cross-talk between HIF and PD-1/PD-L1 pathways in carcinogenesis and therapy. *J Clin Invest* 132: e159473, 2022.
16. Jinushi M, Chiba S, Yoshiyama H, Masutomi K, Kinoshita I, Dosaka-Akita H, Yagita H, Takaoka A and Tahara H: Tumor-associated macrophages regulate tumorigenicity and anticancer drug responses of cancer stem/initiating cells. *Proc Natl Acad Sci USA* 108: 12425-12430, 2011.
17. Saito M, Ichikawa J, Ando T, Schoenecker JG, Ohba T, Koyama K, Suzuki-Inoue K and Haro H: Platelet-derived TGF- $\beta$  induces tissue factor expression via the smad3 pathway in osteosarcoma cells. *J Bone Miner Res* 33: 2048-2058, 2018.
18. Hiratsuka S, Watanabe A, Sakurai Y, Akashi-Takamura S, Ishibashi S, Miyake K, Shibuya M, Akira S, Aburatani H and Maru Y: The S100A8-serum amyloid A3-TLR4 paracrine cascade establishes a pre-metastatic phase. *Nat Cell Biol* 10: 1349-1355, 2008.
19. Liu X, Li J, Yang X, Li X, Kong J, Qi D, Zhang F, Sun B, Liu Y and Liu T: Carcinoma-associated fibroblast-derived lysyl oxidase-rich extracellular vesicles mediate collagen crosslinking and promote epithelial-mesenchymal transition via p-FAK/p-paxillin/YAP signaling. *Int J Oral Sci* 15: 32, 2023.
20. Chevrier S, Crowell HL, Zanotelli VRT, Engler S, Robinson MD and Bodenmiller B: Compensation of signal spillover in suspension and imaging mass cytometry. *Cell Syst* 6: 612-620.e5, 2018.
21. Umezu T, Tadokoro H, Azuma K, Yoshizawa S, Ohyashiki K and Ohyashiki JH: Exosomal miR-135b shed from hypoxic multiple myeloma cells enhances angiogenesis by targeting factor-inhibiting HIF-1. *Blood* 124: 3748-3757, 2014.
22. Principe DR, Kamath SD, Korc M and Munshi HG: The immune modifying effects of chemotherapy and advances in chemo-immunotherapy. *Pharmacol Ther* 236: 108111, 2022.
23. Han C, Liu Z, Zhang Y, Shen A, Dong C, Zhang A, Moore C, Ren Z, Lu C, Cao X, *et al*: Tumor cells suppress radiation-induced immunity by hijacking caspase 9 signaling. *Nat Immunol* 21: 546-554, 2020.
24. Yu Y, Li K, Peng Y, Zhang Z, Pu F, Shao Z and Wu W: Tumor microenvironment in osteosarcoma: From cellular mechanism to clinical therapy. *Genes Dis* 12: 101569, 2025.
25. Dutour A, Pasello M, Farrow L, Amer MH, Entz-Werlé N, Nathrath M, Scotlandi K, Mittnacht S and Gomez-Mascard A: Microenvironment matters: Insights from the FOSTER consortium on microenvironment-driven approaches to osteosarcoma therapy. *Cancer Metastasis Rev* 44: 44, 2025.
26. Azizi E, Carr AJ, Plitas G, Cornish AE, Konopacki C, Prabhakaran S, Nainys J, Wu K, Kiseliovas V and Setty M: Single-Cell map of diverse immune phenotypes in the breast tumor microenvironment. *Cell* 174: 1293-1308.e36, 2018.
27. Sun CY, Zhang Z, Tao L, Xu FF, Li HY, Zhang HY and Liu W: T cell exhaustion drives osteosarcoma pathogenesis. *Ann Transl Med* 9: 1447, 2021.
28. Visser LL, Bleijs M, Margaritis T, van de Wetering M, Holstege FCP and Clevers H: Ewing sarcoma single-cell transcriptome analysis reveals functionally impaired antigen-presenting cells. *Cancer Res Commun* 3: 2158-2169, 2023.
29. Guimarães GR, Maklouf GR, Teixeira CE, de Oliveira Santos L, Tassarollo NG, de Toledo NE, Serain AF, de Lanna CA, Pretti MA, da Cruz JGV, *et al*: Single-cell resolution characterization of myeloid-derived cell states with implication in cancer outcome. *Nat Commun* 15: 5694, 2024.
30. Kashfi K, Kannikal J and Nath N: Macrophage reprogramming and cancer therapeutics: Role of iNOS-Derived NO. *Cells* 10: 3194, 2021.
31. Ka HI, Mun SH, Han S and Yang Y: Targeting myeloid-derived suppressor cells in the tumor microenvironment: Potential therapeutic approaches for osteosarcoma. *Oncol Res* 33: 519-531, 2025.
32. Zhao L, Liu P, Mao M, Zhang S, Bigenwald C, Dutertre CA, Lehmann CHK, Pan H, Paulhan N, Amon L, *et al*: BCL2 inhibition reveals a dendritic cell-specific immune checkpoint that controls tumor immunosurveillance. *Cancer Discov* 13: 2448-2469, 2023.
33. Shaim H, Shanley M, Basar R, Daher M, Gumin J, Zamler DB, Uprety N, Wang F, Huang Y, Gabrusiewicz K, *et al*: Targeting the  $\alpha$ v integrin/TGF- $\beta$  axis improves natural killer cell function against glioblastoma stem cells. *J Clin Invest* 131: e42116, 2021.
34. Tran HC, Wan Z, Sheard MA, Sun J, Jackson JR, Malvar J, Xu Y, Wang L, Sposto R, Kim ES, *et al*: TGF $\beta$ R1 blockade with galunisertib (LY2157299) enhances anti-neuroblastoma activity of the anti-GD2 antibody dinutuximab (ch14.18) with natural killer cells. *Clin Cancer Res* 23: 804-813, 2017.
35. Cao JW, Lake J, Impastato R, Chow L, Perez L, Chubb L, Kurihara J, Verneris MR and Dow S: Targeting osteosarcoma with canine B7-H3 CAR T cells and impact of CXCR2 Co-expression on functional activity. *Cancer Immunol Immunother* 73: 77, 2024.
36. Zhang Q, Zhang Z, Liu G, Li D, Gu Z, Zhang L, Pan Y, Cui X, Wang L, Liu G, *et al*: B7-H3 targeted CAR-T cells show highly efficient anti-tumor function against osteosarcoma both in vitro and in vivo. *BMC Cancer* 22: 1124, 2022.
37. Fotsitzoudis C, Koulouridi A, Messaritakis I, Konstantinidis T, Gouvas N, Tsiaoussis J and Souglakos J: Cancer-associated fibroblasts: The origin, biological characteristics and role in cancer-a glance on colorectal cancer. *Cancers (Basel)* 14: 4394, 2022.
38. Cao Z, Quazi S, Arora S, Osellame LD, Burvenich IJ, Janes PW and Scott AM: Cancer-associated fibroblasts as therapeutic targets for cancer: Advances, challenges, and future prospects. *J Biomed Sci* 32: 7, 2025.
39. Long AH, Highfill SL, Cui Y, Smith JP, Walker AJ, Ramakrishna S, El-Etriby R, Galli S, Tsokos MG, Orentas RJ and Mackall CL: Reduction of MDSCs with all-trans retinoic acid improves CAR therapy efficacy for sarcomas. *Cancer Immunol Res* 4: 869-880, 2016.
40. Calvi LM, Adams GB, Weibrecht KW, Weber JM, Olson DP, Knight MC, Martin RP, Schipani E, Divieti P, Bringhurst FR, *et al*: Osteoblastic cells regulate the haematopoietic stem cell niche. *Nature* 425: 841-846, 2003.
41. Wang S, Greenbaum J, Qiu C, Gong Y, Wang Z, Lin X, Liu Y, He P, Meng X, Zhang Q, *et al*: Single-cell RNA sequencing reveals in vivo osteoimmunology interactions between the immune and skeletal systems. *Front Endocrinol (Lausanne)* 14: 1107511, 2023.
42. Canon JR, Roudier M, Bryant R, Morony S, Stolina M, Kostenuik PJ and Dougall WC: Inhibition of RANKL blocks skeletal tumor progression and improves survival in a mouse model of breast cancer bone metastasis. *Clin Exp Metastasis* 25: 119-129, 2008.
43. Kiesel JR, Buchwald ZS and Aurora R: Cross-presentation by osteoclasts induces FoxP3 in CD8+ T cells. *J Immunol* 182: 5477-5487, 2009.

44. Panagi M, Mpekris F, Voutouri C, Hadjigeorgiou AG, Symeonidou C, Porfyriou E, Michael C, Stylianou A, Martin JD, Cabral H, *et al*: Stabilizing tumor-resident mast cells restores T-cell infiltration and sensitizes sarcomas to PD-L1 inhibition. *Clin Cancer Res* 30: 2582-2597, 2024.
45. Białas M, Dyduch G, Dudała J, Bereza-Buziak M, Hubalewska-Dydejczyk A, Budzyński A and Okoń K: Study of microvessel density and the expression of vascular endothelial growth factors in adrenal gland pheochromocytomas. *Int J Endocrinol* 2014: 104129, 2014.
46. Kreisl TN, Kim L, Moore K, Duic P, Royce C, Stroud I, Garren N, Mackey M, Butman JA and Camphausen K: Phase II trial of single-agent bevacizumab followed by bevacizumab plus irinotecan at tumor progression in recurrent glioblastoma. *J Clin Oncol* 27: 740-745, 2009.
47. Dong X, Ren J, Amoozgar Z, Lee S, Datta M, Roberge S, Duquette M, Fukumura D and Jain RK: Anti-VEGF therapy improves EGFR-vIII-CAR-T cell delivery and efficacy in syngeneic glioblastoma models in mice. *J Immunother Cancer* 11: e005583, 2023.
48. Karnoub AE, Dash AB, Vo AP, Sullivan A, Brooks MW, Bell GW, Richardson AL, Polyak K, Tubo R and Weinberg RA: Mesenchymal stem cells within tumour stroma promote breast cancer metastasis. *Nature* 449: 557-563, 2007.
49. Trabanelli S, Lecciso M, Salvestrini V, Cavo M, Očadlíková D, Lemoli RM and Curti A: PGE2-induced IDO1 inhibits the capacity of fully mature DCs to elicit an in vitro antileukemic immune response. *J Immunol Res* 2015: 253191, 2015.
50. Zelenay S, van der Veen AG, Böttcher JP, Snelgrove KJ, Rogers N, Acton SE, Chakravarty P, Girotti MR, Marais R, Quezada SA, *et al*: Cyclooxygenase-dependent tumor growth through evasion of immunity. *Cell* 162: 1257-1270, 2015.
51. Kolb AD and Bussard KM: The bone extracellular matrix as an ideal milieu for cancer cell metastases. *Cancers (Basel)* 11: 1020, 2019.
52. Molina ER, Chim LK, Salazar MC, Mehta SM, Menegaz BA, Lamhamedi-Cherradi SE, Satish T, Mohiuddin S, McCall D, Zaske AM, *et al*: Mechanically tunable coaxial electrospun models of YAP/TAZ mechanoresponse and IGF-1R activation in osteosarcoma. *Acta Biomater* 100: 38-51, 2019.
53. Liu D, Peng Y, Li X, Zhu Z, Mi Z, Zhang Z and Fan H: Comprehensive landscape of TGFβ-related signature in osteosarcoma for predicting prognosis, immune characteristics, and therapeutic response. *J Bone Oncol* 40: 100484, 2023.
54. Highfill SL, Cui Y, Giles AJ, Smith JP, Zhang H, Morse E, Kaplan RN and Mackall CL: Disruption of CXCR2-mediated MDSC tumor trafficking enhances anti-PD1 efficacy. *Sci Transl Med* 6: 237ra67, 2014.
55. Zhao TT, Zhou TJ, Zhang C, Liu YX, Wang WJ, Li C, Xing L and Jiang HL: Hypoxia inhibitor combined with chemotherapeutic agents for antitumor and antimetastatic efficacy against osteosarcoma. *Mol Pharm* 20: 2612-2623, 2023.
56. Khojastehzhad MA, Seyedi SMR, Raoufi F and Asoodeh A: Association of hypoxia-inducible factor 1 expressions with prognosis role as a survival prognostic biomarker in the patients with osteosarcoma: A meta-analysis. *Expert Rev Mol Diagn* 22: 1099-1106, 2022.
57. Shi W, Cassmann TJ, Bhagwate AV, Hitosugi T and Ip WKE: Lactic acid induces transcriptional repression of macrophage inflammatory response via histone acetylation. *Cell Rep* 43: 113746, 2024.
58. Hashim AI, Cornell HH, Mde LC, Abrahams D, Cunningham J, Lloyd M, Martinez GV, Gatenby RA and Gillies RJ: Reduction of metastasis using a non-volatile buffer. *Clin Exp Metastasis* 28: 841-849, 2011.
59. Aquino A and Franzese O: Reciprocal modulation of tumour and immune cell motility: Uncovering dynamic interplays and therapeutic approaches. *Cancers (Basel)* 17: 1547, 2025.
60. Cui J, Dean D, Hornicek FJ, Chen Z and Duan Z: The role of extracellular matrix in osteosarcoma progression and metastasis. *J Exp Clin Cancer Res* 39: 178, 2020.
61. Liu W, Hu H, Shao Z, Lv X, Zhang Z, Deng X, Song Q, Han Y, Guo T, Xiong L, *et al*: Characterizing the tumor microenvironment at the single-cell level reveals a novel immune evasion mechanism in osteosarcoma. *Bone Res* 11: 4, 2023.
62. Gorchs L, Oosthoek M, Yucel-Lindberg T, Moro CF and Kaiphe H: Chemokine receptor expression on T cells is modulated by CAFs and chemokines affect the spatial distribution of T cells in pancreatic tumors. *Cancers (Basel)* 14: 3826, 2022.
63. Park HK, Kim M, Sung M, Lee SE, Kim YJ and Choi YL: Status of programmed death-ligand 1 expression in sarcomas. *J Transl Med* 16: 303, 2018.
64. Yang R, Sun L, Li CF, Wang YH, Yao J, Li H, Yan M, Chang WC, Hsu JM, Cha JH, *et al*: Galectin-9 interacts with PD-1 and TIM-3 to regulate T cell death and is a target for cancer immunotherapy. *Nat Commun* 12: 832, 2021.
65. Selby MJ, Engelhardt JJ, Quigley M, Henning KA, Chen T, Srinivasan M and Korman AJ: Anti-CTLA-4 antibodies of IgG2a isotype enhance antitumor activity through reduction of intratumoral regulatory T cells. *Cancer Immunol Res* 1: 32-42, 2013.
66. Jiang X, Li L, Li Y and Li Q: Molecular mechanisms and countermeasures of immunotherapy resistance in malignant tumor. *J Cancer* 10: 1764-1771, 2019.
67. Tian H, Cao J, Li B, Nice EC, Mao H, Zhang Y and Huang C: Managing the immune microenvironment of osteosarcoma: The outlook for osteosarcoma treatment. *Bone Res* 11: 11, 2023.
68. Starska-Kowarska K: The role of different immunocompetent cell populations in the pathogenesis of head and neck cancer-regulatory mechanisms of pro- and anti-cancer activity and their impact on immunotherapy. *Cancers (Basel)* 15: 1642, 2023.
69. Li C, Jiang P, Wei S, Xu X and Wang J: Regulatory T cells in tumor microenvironment: New mechanisms, potential therapeutic strategies and future prospects. *Mol Cancer* 19: 116, 2020.
70. Denize T, Jegede OA, Matar S, El Ahmar N, West DJ, Walton E, Bagheri AS, Savla V, Laimon YN, Gupta S, *et al*: PD-1 expression on intratumoral regulatory T cells is associated with lack of benefit from Anti-PD-1 therapy in metastatic clear-cell renal cell carcinoma patients. *Clin Cancer Res* 30: 803-813, 2024.
71. Merchant MS, Melchionda F, Sinha M, Khanna C, Helman L and Mackall CL: Immune reconstitution prevents metastatic recurrence of murine osteosarcoma. *Cancer Immunol Immunother* 56: 1037-1046, 2007.
72. Han Q, Shi H and Liu F: CD163(+) M2-type tumor-associated macrophage support the suppression of tumor-infiltrating T cells in osteosarcoma. *Int Immunopharmacol* 34: 101-106, 2016.
73. Gallina G, Dolcetti L, Serafini P, De Santo C, Marigo I, Colombo MP, Basso G, Brombacher F, Borrello I, Zanovello P, *et al*: Tumors induce a subset of inflammatory monocytes with immunosuppressive activity on CD8+ T cells. *J Clin Invest* 116: 2777-2790, 2006.
74. Munder M: Arginase: An emerging key player in the mammalian immune system. *Br J Pharmacol* 158: 638-651, 2009.
75. Yang Y, Li C, Liu T, Dai X and Bazhin AV: Myeloid-derived suppressor cells in tumors: from mechanisms to antigen specificity and microenvironmental regulation. *Front Immunol* 11: 1371, 2020.
76. Zhu Y, Knolhoff BL, Meyer MA, Nywening TM, West BL, Luo J, Wang-Gillam A, Goedegebuure SP, Linehan DC and DeNardo DG: CSF1/CSF1R blockade reprograms tumor-infiltrating macrophages and improves response to T-cell checkpoint immunotherapy in pancreatic cancer models. *Cancer Res* 74: 5057-5069, 2014.
77. DeNardo DG, Brennan DJ, Rexhepaj E, Ruffell B, Shiao SL, Madden SF, Gallagher WM, Wadhwani N, Keil SD, Junaid SA, *et al*: Leukocyte complexity predicts breast cancer survival and functionally regulates response to chemotherapy. *Cancer Discov* 1: 54-67, 2011.
78. Hashimoto M, Kamphorst AO, Im SJ, Kissick HT, Pillai RN, Ramalingam SS, Araki K and Ahmed R: CD8 T cell exhaustion in chronic infection and cancer: Opportunities for interventions. *Annu Rev Med* 69: 301-318, 2018.
79. Depuydt MAC, Schaftenaar FH, Prange KHM, Boltjes A, Hemme E, Delfos L, de Mol J, de Jong MJM, Kleijn MNA, Peeters JAHM, *et al*: Single-cell T cell receptor sequencing of paired human atherosclerotic plaques and blood reveals autoimmune-like features of expanded effector T cells. *Nat Cardiovasc Res* 2: 112-125, 2023.
80. Shin J, O'Brien TF, Grayson JM and Zhong XP: Differential regulation of primary and memory CD8 T cell immune responses by diacylglycerol kinases. *J Immunol* 188: 2111-2117, 2012.
81. Gu XY, Yang JL, Lai R, Zhou ZJ, Tang D, Hu L and Zhao LJ: Impact of lactate on immune cell function in the tumor microenvironment: Mechanisms and therapeutic perspectives. *Front Immunol* 16: 1563303, 2025.
82. Leone RD, Sun IM, Oh MH, Sun IH, Wen J, Englert J and Powell JD: Inhibition of the adenosine A2a receptor modulates expression of T cell coinhibitory receptors and improves effector function for enhanced checkpoint blockade and ACT in murine cancer models. *Cancer Immunol Immunother* 67: 1271-1284, 2018.

83. Heger L, Hatscher L, Liang C, Lehmann CHK, Amon L, Lühr JJ, Kaszubowski T, Nzirorera R, Schaft N, Dörrle J, *et al*: XCR1 expression distinguishes human conventional dendritic cell type 1 with full effector functions from their immediate precursors. *Proc Natl Acad Sci USA* 120: e2300343120, 2023.
84. Ohno Y, Kitamura H, Takahashi N, Ohtake J, Kaneumi S, Sumida K, Homma S, Kawamura H, Minagawa N, Shibasaki S and Taketomi A: IL-6 down-regulates HLA class II expression and IL-12 production of human dendritic cells to impair activation of antigen-specific CD4(+) T cells. *Cancer Immunol Immunother* 65: 193-204, 2016.
85. Oba T, Long MD, Keler T, Marsh HC, Minderman H, Abrams SI, Liu S and Ito F: Overcoming primary and acquired resistance to anti-PD-L1 therapy by induction and activation of tumor-residing cDC1s. *Nat Commun* 11: 5415, 2020.
86. Ying H, Li ZQ, Li MP and Liu WC: Metabolism and senescence in the immune microenvironment of osteosarcoma: Focus on new therapeutic strategies. *Front Endocrinol (Lausanne)* 14: 1217669, 2023.
87. Bogdanov A, Bogdanov A, Chubenko V, Volkov N, Moiseenko F and Moiseyenko V: Tumor acidity: From hallmark of cancer to target of treatment. *Front Oncol* 12: 979154, 2022.
88. Muller AJ, DuHadaway JB, Donover PS, Sutanto-Ward E and Prendergast GC: Inhibition of indoleamine 2,3-dioxygenase, an immunoregulatory target of the cancer suppression gene Bin1, potentiates cancer chemotherapy. *Nat Med* 11: 312-319, 2005.
89. Bopp T, Becker C, Klein M, Klein-Hessling S, Palmethofer A, Serfling E, Heib V, Becker M, Kubach J, Schmitt S, *et al*: Cyclic adenosine monophosphate is a key component of regulatory T cell-mediated suppression. *J Exp Med* 204: 1303-1310, 2007.
90. Ji Y, Xiao C, Fan T, Deng Z, Wang D, Cai W, Li J, Liao T, Li C and He J: The epigenetic hallmarks of immune cells in cancer. *Mol Cancer* 24: 66, 2025.
91. Liu W, Long Q, Zhang W, Zeng D, Hu B, Liu S and Chen L: miRNA-221-3p derived from M2-polarized tumor-associated macrophage exosomes aggravates the growth and metastasis of osteosarcoma through SOCS3/JAK2/STAT3 axis. *Aging (Albany NY)* 13: 19760-19775, 2021.
92. Hou Y, Zak J, Shi Y, Pratumchai I, Dinner B, Wang W, Qin K, Weber EW, Teijaro JR and Wu P: Transient EZH2 suppression by tazemetostat during in vitro expansion maintains T-cell stemness and improves adoptive T-cell therapy. *Cancer Immunol Res* 13: 47-65, 2025.
93. Tawbi HA, Burgess M, Bolejack V, Van Tine BA, Schuetz SM, Hu J, D'Angelo S, Attia S, Riedel RF, Priebe DA, *et al*: Pembrolizumab in advanced soft-tissue sarcoma and bone sarcoma (SARC028): A multicentre, two-cohort, single-arm, open-label, phase 2 trial. *Lancet Oncol* 18: 1493-1501, 2017.
94. Le Cesne A, Marec-Berard P, Blay JY, Gaspar N, Bertucci F, Penel N, Bompas E, Cousin S, Toulmonde M, Bessede A, *et al*: Programmed cell death 1 (PD-1) targeting in patients with advanced osteosarcomas: Results from the PEMBROSARC study. *Eur J Cancer* 119: 151-157, 2019.
95. Davis KL, Fox E, Merchant MS, Reid JM, Kudgus RA, Liu X, Minard CG, Voss S, Berg SL, Weigel BJ and Mackall CL: Nivolumab in children and young adults with relapsed or refractory solid tumours or lymphoma (ADVL1412): A multicentre, open-label, single-arm, phase 1-2 trial. *Lancet Oncol* 21: 541-550, 2020.
96. Davis KL, Fox E, Isikwei E, Reid JM, Liu X, Minard CG, Voss S, Berg SL, Weigel BJ and Mackall CL: A phase I/II trial of nivolumab plus ipilimumab in children and young adults with relapsed/refractory solid tumors: A children's oncology group study ADVL1412. *Clin Cancer Res* 28: 5088-5097, 2022.
97. Boye K, Longhi A, Guren T, Lorenz S, Næss S, Pierini M, Taksdal I, Lobmaier I, Cesari M, Paioli A, *et al*: Pembrolizumab in advanced osteosarcoma: Results of a single-arm, open-label, phase 2 trial. *Cancer Immunol Immunother* 70: 2617-2624, 2021.
98. Palmerini E, Pousa AL, Grignani G, Redondo A, Hindi N, Provenzano S, Sebbo A, Martin JA, Valverde C, Trufero JM, *et al*: Nivolumab and sunitinib in patients with advanced bone sarcomas: A multicenter, single-arm, phase 2 trial. *Cancer* 131: e35628, 2025.
99. Yang C, Lai Y, Wang J, Chen Q, Pan Q, Xu C, Mo P, Guo G, Chen R, Liu N and Wu Y: Spatial heterogeneity of PD-1/PD-L1 defined osteosarcoma microenvironments at single-cell spatial resolution. *Lab Invest* 104: 102143, 2024.
100. Jiang K, Li J, Zhang J, Wang L, Zhang Q, Ge J, Guo Y, Wang B, Huang Y, Yang T, *et al*: SDF-1/CXCR4 axis facilitates myeloid-derived suppressor cells accumulation in osteosarcoma microenvironment and blunts the response to anti-PD-1 therapy. *Int Immunopharmacol* 75: 105818, 2019.
101. Toda Y, Kohashi K, Yamada Y, Yoshimoto M, Ishihara S, Ito Y, Iwasaki T, Yamamoto H, Matsumoto Y and Nakashima Y: PD-L1 and IDO1 expression and tumor-infiltrating lymphocytes in osteosarcoma patients: Comparative study of primary and metastatic lesions. *J Cancer Res Clin Oncol* 146: 2607-2620, 2020.
102. Ribatti D: Mast cells and resistance to immunotherapy in cancer. *Arch Immunol Ther Exp (Warsz)* 71: 11, 2023.
103. Lee AQ, Hao C, Pan M, Ganjoo KN and Bui NQ: Histologic and immunologic factors associated with response to immune checkpoint inhibitors in advanced sarcoma. *Clin Cancer Res* 31: 678-684, 2025.
104. Huang X, Park H, Greene J, Pao J, Mulvey E, Zhou SX, Albert CM, Moy F, Sachdev D, Yee D, *et al*: IGF1R- and ROR1-Specific CAR T cells as a potential therapy for high risk sarcomas. *PLoS One* 10: e0133152, 2015.
105. Majzner RG, Theruvath JL, Nellan A, Heitzeneder S, Cui Y, Mount CW, Rietberg SP, Linde MH, Xu P, Rota C, *et al*: CAR T cells targeting B7-H3, a pan-cancer antigen, demonstrate potent preclinical activity against pediatric solid tumors and brain tumors. *Clin Cancer Res* 25: 2560-2574, 2019.
106. Talbot LJ, Chabot A, Funk A, Nguyen P, Wagner J, Ross A, Tillman H, Davidoff A, Gottschalk S and DeRenzo C: A novel orthotopic implantation technique for osteosarcoma produces spontaneous metastases and illustrates dose-dependent efficacy of B7-H3-CAR T cells. *Front Immunol* 12: 691741, 2021.
107. Lake JA, Woods E, Hoffmeyer E, Schaller KL, Cruz-Cruz J, Fernandez J, Tufa D, Kooiman B, Hall SC, Jones D, *et al*: Directing B7-H3 chimeric antigen receptor T cell homing through IL-8 induces potent antitumor activity against pediatric sarcoma. *J Immunother Cancer* 12: e009221, 2024.
108. Talbot LJ, Chabot A, Ross AB, Beckett A, Nguyen P, Fleming A, Chockley PJ, Sheppard H, Wang J, Gottschalk S and DeRenzo C: Redirecting B7-H3.CAR T cells to chemokines expressed in osteosarcoma enhances homing and antitumor activity in preclinical models. *Clin Cancer Res* 30: 4434-4449, 2024.
109. Wang Y, Yu W, Zhu J, Wang J, Xia K, Liang C and Tao H: Anti-CD166/4-1BB chimeric antigen receptor T cell therapy for the treatment of osteosarcoma. *J Exp Clin Cancer Res* 38: 168, 2019.
110. Charan M, Dravid P, Cam M, Audino A, Gross AC, Arnold MA, Roberts RD, Cripe TP, Pertsemelidis A, Houghton PJ and Cam H: GD2-directed CAR-T cells in combination with HGF-targeted neutralizing antibody (AMG102) prevent primary tumor growth and metastasis in Ewing sarcoma. *Int J Cancer* 146: 3184-3195, 2020.
111. Englisch A, Altvater B, Kailayangiri S, Hartmann W and Rossig C: VEGFR2 as a target for CAR T cell therapy of Ewing sarcoma. *Pediatr Blood Cancer* 67: e28313, 2020.
112. Hsu K, Middlemiss S, Saletta F, Gottschalk S, McCowage GB and Kramer B: Chimeric antigen receptor-modified T cells targeting EphA2 for the immunotherapy of paediatric bone tumours. *Cancer Gene Ther* 28: 321-334, 2021.
113. Lu YJ, Chu H, Wheeler LW, Nelson M, Westrick E, Matthaei JF, Cardle II, Johnson A, Gustafson J, Parker N, *et al*: Preclinical evaluation of bispecific adaptor molecule controlled folate receptor CAR-T cell therapy with special focus on pediatric malignancies. *Front Oncol* 9: 151, 2019.
114. Watanabe Y, Tsukahara T, Murata K, Hamada S, Kubo T, Kanaseki T, Hirohashi Y, Emori M, Teramoto A, Nakatsugawa M, *et al*: Development of CAR-T cells specifically targeting cancer stem cell antigen DNAJB8 against solid tumours. *Br J Cancer* 128: 886-895, 2023.
115. Mensali N, Köksal H, Joaquina S, Wernhoff P, Casey NP, Romecin P, Panisello C, Rodriguez R, Vimeux L, Juzeniene A, *et al*: ALPL-1 is a target for chimeric antigen receptor therapy in osteosarcoma. *Nat Commun* 14: 3375, 2023.
116. Wickman E, Lange S, Wagner J, Ibanez J, Tian L, Lu M, Sheppard H, Chiang J, Koo SC, Vogel P, *et al*: IL-18R supported CAR T cells targeting oncofetal tenascin C for the immunotherapy of pediatric sarcoma and brain tumors. *J Immunother Cancer* 12: e009743, 2024.
117. Hu J, Yang Q, Zhang W, Du H, Chen Y, Zhao Q, Dao L, Xia X, Wall FN, Zhang Z, *et al*: Cell membrane-anchored and tumor-targeted IL-12 (attIL12)-T cell therapy for eliminating large and heterogeneous solid tumors. *J Immunother Cancer* 10: e003633, 2022.
118. Yang Q, Hu J, Jia Z, Wang Q, Wang J, Dao LH, Zhang W, Zhang S, Xia X, Gorlick R and Li S: Membrane-anchored and tumor-targeted IL12 (attIL12)-PBMC therapy for osteosarcoma. *Clin Cancer Res* 28: 3862-3873, 2022.

119. Hui X, Farooq MA, Chen Y, Ajmal I, Ren Y, Xue M, Ji Y, Du B, Wu S and Jiang W: A novel strategy of co-expressing CXCR5 and IL-7 enhances CAR-T cell effectiveness in osteosarcoma. *Front Immunol* 15: 1462076, 2024.
120. Adeshakin AO, Shi H, Perry SS, Sheppard H, Nguyen P, Sun X, Zhou P, Métais JY, Cunningham T, Anil KC, *et al*: Targeting Regnase-1 unleashes CAR T cell antitumor activity for osteosarcoma and creates a proinflammatory tumor microenvironment. *bioRxiv* 23: 2025.05.20.650777, 2025.
121. Hidalgo L, Somovilla-Crespo B, Garcia-Rodriguez P, Morales-Molina A, Rodriguez-Milla MA and Garcia-Castro J: Switchable CAR T cell strategy against osteosarcoma. *Cancer Immunol Immunother* 72: 2623-2633, 2023.
122. Wang Z, Yan N, Sheng H, Xiao Y, Sun J and Cao C: Single-cell transcriptomic analysis reveals an immunosuppressive network between POSTN CAFs and ACKR1 ECs in TKI-resistant lung cancer. *Cancer Genomics Proteomics* 21: 65-78, 2024.
123. Altvater B, Kailayangiri S, Lanuza LF, Urban K, Greune L, Flügge M, Meltzer J, Farwick N, König S, Görlich D, *et al*: HLA-G and HLA-E immune checkpoints are widely expressed in ewing sarcoma but have limited functional impact on the effector functions of antigen-specific CAR T cells. *Cancers (Basel)* 13: 2857, 2021.
124. Pezzella M, Quintarelli C, Quadraccia MC, Sarcinelli A, Manni S, Iaffaldano L, Ottaviani A, Ciccone R, Camera A, D'Amore ML, *et al*: Tumor-derived G-CSF induces an immunosuppressive microenvironment in an osteosarcoma model, reducing response to CAR.GD2 T-cells. *J Hematol Oncol* 17: 127, 2024.
125. Kaczanowska S, Murty T, Alimadadi A, Contreras CF, Duault C, Subrahmanyam PB, Reynolds W, Gutierrez NA, Baskar R, Wu CJ, *et al*: Immune determinants of CAR-T cell expansion in solid tumor patients receiving GD2 CAR-T cell therapy. *Cancer Cell* 42: 35-51.e8, 2024.
126. Arnett AB and Heczey A: GD2-CAR CAR T cells in patients with osteosarcoma and neuroblastoma-it's not only the T cells that matter. *Cancer Cell* 42: 8-10, 2024.
127. Lu YC, Parker LL, Lu T, Zheng Z, Toomey MA, White DE, Yao X, Li YF, Robbins PF, Feldman SA, *et al*: Treatment of patients with metastatic cancer using a major histocompatibility complex class II-restricted T-cell receptor targeting the cancer germline antigen MAGE-A3. *J Clin Oncol* 35: 3322-3329, 2017.
128. Hamada S, Tsukahara T, Watanabe Y, Murata K, Mizue Y, Kubo T, Kanaseki T, Hirohashi Y, Emori M, Nakatsugawa M, *et al*: Development of T cell receptor-engineered T cells targeting the sarcoma-associated antigen papillomavirus binding factor. *Cancer Sci* 115: 24-35, 2024.
129. Ketola A, Hinkkanen A, Yongabi F, Furu P, Määttä AM, Liimatainen T, Pirinen R, Björn M, Hakkarainen T, Mäkinen K, *et al*: Oncolytic Semliki forest virus vector as a novel candidate against unresectable osteosarcoma. *Cancer Res* 68: 8342-8350, 2008.
130. Hingorani P, Zhang W, Lin J, Liu L, Guha C and Kolb EA: Systemic administration of reovirus (Reolysin) inhibits growth of human sarcoma xenografts. *Cancer* 117: 1764-1774, 2011.
131. Christie JD, Appel N, Zhang L, Lowe K, Kilbourne J, Daggett-Vondras J, Elliott N, Lucas AR, Blattman JN, Rahman MM and McFadden G: Systemic delivery of mLIGHT-armed myxoma virus is therapeutic for later-stage syngeneic murine lung metastatic osteosarcoma. *Cancers (Basel)* 14: 337, 2022.
132. Laborda E, Puig-Saus C, Rodriguez-García A, Moreno R, Cascalló M, Pastor J and Alemany R: A pRb-responsive, RGD-modified, and hyaluronidase-armed canine oncolytic adenovirus for application in veterinary oncology. *Mol Ther* 22: 986-998, 2014.
133. Musser ML, Berger EP, Tripp CD, Clifford CA, Bergman PJ and Johannes CM: Safety evaluation of the canine osteosarcoma vaccine, live *Listeria* vector. *Vet Comp Oncol* 19: 92-98, 2021.
134. Chen A, Qiu Y, Yen YT, Wang C, Wang X, Li C, Wei Z, Li L, Yu L, Liu F and Li R: Expression of cancer-testis antigens MAGE-A1, MAGE-A4, NY-ESO-1 and PRAME in bone and soft tissue sarcomas: The experience from a single center in China. *Cancer Med* 14: e70750, 2025.
135. Gu J, Ji Z, Li D and Dong Q: Proliferation inhibition and apoptosis promotion by dual silencing of VEGF and Survivin in human osteosarcoma. *Acta Biochim Biophys Sin (Shanghai)* 51: 59-67, 2019.
136. Zhang Y, Cheng H, Li W, Wu H and Yang Y: Highly-expressed P2X7 receptor promotes growth and metastasis of human HOS/MNNG osteosarcoma cells via PI3K/Akt/GSK3 $\beta$ / $\beta$ -catenin and mTOR/HIF1 $\alpha$ /VEGF signaling. *Int J Cancer* 145: 1068-1082, 2019.
137. Dong J, Chai X, Xue Y, Shen S, Chen Z, Wang Z, Yinwang E, Wang S, Chen L, Wu F, *et al*: ZIF-8-encapsulated pexidartinib delivery via targeted peptide-modified M1 macrophages attenuates MDSC-mediated immunosuppression in osteosarcoma. *Small* 20: e2309038, 2024.
138. Gutiérrez LM, Alvarez MV, Yang Y, Spinelli F, Cantero MJ, Alaniz L, García MG, Kleinerman ES, Correa A and Bolontrade MF: Up-regulation of pro-angiogenic molecules and events does not relate with an angiogenic switch in metastatic osteosarcoma cells but to cell survival features. *Apoptosis* 26: 447-459, 2021.
139. LShijie L, Zhen P, Kang Q, Hua G, Qingcheng Y and Dongdong C: Deregulation of CLTC interacts with TFG, facilitating osteosarcoma via the TGF-beta and AKT/mTOR signaling pathways. *Clin Transl Med* 11: e377, 2021.
140. Xie L, Liang X, Xu J, Sun X, Liu K, Sun K, Li Y, Tang X, Li X, Zhan X, *et al*: Exploratory study of an anti-PD-L1/TGF- $\beta$  antibody, TQB2858, in patients with refractory or recurrent osteosarcoma and alveolar soft part sarcoma: A report from Chinese sarcoma study group (TQB2858-1b-02). *BMC Cancer* 23: 868, 2023.
141. Hu J, Lazar AJ, Ingram D, Wang WL, Zhang W, Jia Z, Ragoonanan D, Wang J, Xia X, Mahadeo K, *et al*: Cell membrane-anchored and tumor-targeted IL-12 T-cell therapy destroys cancer-associated fibroblasts and disrupts extracellular matrix in heterogenous osteosarcoma xenograft models. *J Immunother Cancer* 12: e006991, 2024.
142. Kong D, Ying B, Zhang J and Ying H: The anti-osteosarcoma property of ailanthone through regulation of miR-126/VEGF-A axis. *Artif Cells Nanomed Biotechnol* 47: 3913-3919, 2019.
143. Li B, Dang X, Duan J, Zhang G, Zhang J and Song Q: SIX4 upregulates IDH1 and metabolic reprogramming to promote osteosarcoma progression. *J Cell Mol Med* 27: 259-265, 2023.
144. Shan J, Lin Z, Rashid H, Huang P, Qiang L, Liu Y, Shen G, Li Y, Cui J, Su Z, *et al*: A novel therapeutic strategy for osteosarcoma using anti-GD2 ADC and EZH2 inhibitor. *Biomark Res* 13: 87, 2025.
145. Taylor AM, Sheng J, Ng PKS, Harder JM, Kumar P, Ahn JY, Cao Y, Dzis AM, Jillette NL, Goodspeed A, *et al*: Immunosuppressive tumor microenvironment of osteosarcoma. *Cancers (Basel)* 17: 2117, 2025.
146. Gassmann H, Schneider K, Evdokimova V, Ruzanov P, Schober SJ, Xue B, von Heyking K, Thiede M, Richter GHS, Pfaffl MW, *et al*: Ewing sarcoma-derived extracellular vesicles impair dendritic cell maturation and function. *Cells* 10: 2081, 2021.
147. Wang L, Dou X, Xie L, Zhou X, Liu Y, Liu J and Liu X: Metabolic landscape of osteosarcoma: Reprogramming of lactic acid metabolism and metabolic communication. *Front Biosci (Landmark Ed)* 29: 83, 2024.
148. Wang Y, Wang X, Liu Y, Xu J, Zhu J, Zheng Y and Qi Q: A novel hypoxia- and lactate metabolism-related prognostic signature to characterize the immune landscape and predict immunotherapy response in osteosarcoma. *Front Immunol* 15: 1467052, 2024.
149. Zhu J, Simayi N, Wan R and Huang W: CAR T targets and microenvironmental barriers of osteosarcoma. *Cytotherapy* 24: 567-576, 2022.
150. Nguyen DT, Ogando-Rivas E, Liu R, Wang T, Rubin J, Jin L, Tao H, Sawyer WW, Mendez-Gomez HR, Cascio M, *et al*: CAR T cell locomotion in solid tumor microenvironment. *Cells* 11: 1974, 2022.
151. Chim LK, Williams IL, Bashor CJ and Mikos AG: Tumor-associated macrophages induce inflammation and drug resistance in a mechanically tunable engineered model of osteosarcoma. *Biomaterials* 296: 122076, 2023.
152. Cheng JN, Jin Z, Su C, Jiang T, Zheng X, Guo J, Li X, Chu H, Jia J, Zhou Q, *et al*: Bone metastases diminish extraosseous response to checkpoint blockade immunotherapy through osteopontin-producing osteoclasts. *Cancer Cell* 43: 1093-1107.e9, 2025.
153. Martinov T, McKenna KM, Tan WH, Collins EJ, Kehret AR, Linton JD, Olsen TM, Shobaki N and Rongvaux A: Building the next generation of humanized hematopoietic-lymphoid system mice. *Front Immunol* 12: 643852, 2021.
154. Yin L, Wang XJ, Chen DX, Liu XN and Wang XJ: Humanized mouse model: A review on preclinical applications for cancer immunotherapy. *Am J Cancer Res* 10: 4568-4584, 2020.
155. Bacac M, Klein C and Umana P: CEA TCB: A novel head-to-tail 2:1 T cell bispecific antibody for treatment of CEA-positive solid tumors. *Oncoimmunology* 5: e1203498, 2016.

156. Lehmann S, Perera R, Grimm HP, Sam J, Colombetti S, Fauti T, Fahrni L, Schaller T, Freimoser-Grundschober A, Zielonka J, *et al.*: In vivo fluorescence imaging of the activity of CEA TCB, a novel T-Cell bispecific antibody, reveals highly specific tumor targeting and fast induction of T-Cell-mediated tumor killing. *Clin Cancer Res* 22: 4417-4427, 2016.
157. Sun Z, Gu M, Yang Z, Shi L, Zhao L, Zheng M, Wang Y, Zhang W, Han K and Tang N: Application of humanized mice in the safety experiments of antibody drugs. *Animal Model Exp Med* 8: 1023-1032, 2025.
158. Gail LM, Schell KJ, Łacina P, Strobl J, Bolton SJ, Ulriksen ES, Bogunia-Kubik K, Greinix H, Crossland RE, Inngjerdingen M and Stary G: Complex interactions of cellular players in chronic Graft-versus-Host Disease. *Front Immunol* 14: 1199422, 2023.
159. Jackett KN, DaPonte DL, Soman P and Horton JA: Modeling the effects of radiation on the bone tumor microenvironment: Opportunities for exploring combination therapies in microphysiologic systems. *Cell Mol Biol Lett* 30: 97, 2025.
160. Zheng BW, Zheng BY, Niu HQ, Yang YF, Zhu GQ, Li J, Zhang TL and Zou MX: Tumor growth rate in spinal giant cell tumors of bone and association with the immune microenvironment and denosumab treatment responsiveness: A multicenter study. *Neurosurgery* 92: 524-537, 2023.
161. Cheng X, Peng T, Chu T, Yang Y, Liu J, Gao Q, Cao C and Wei J: Application of single-cell and spatial omics in deciphering cellular hallmarks of cancer drug response and resistance. *J Hematol Oncol* 18: 70, 2025.
162. Chen J, Chen F, Zhang H, Hu Y, Zhou X, Weng X, Bao G and Ding X: Multi-omics-based construction of a palmitoylation-driven prognostic model reveals tumor immune phenotypes in osteosarcoma. *Discov Oncol* 16: 1544, 2025.
163. Yu B, Pacureanu A, Olivier C, Cloetens P and Peyrin F: Assessment of the human bone lacuno-canalicular network at the nanoscale and impact of spatial resolution. *Sci Rep* 10: 4567, 2020.
164. Lu T, Park S, Zhu J, Wang Y, Zhan X, Wang X, Wang L, Zhu H and Wang T: Overcoming Expressional drop-outs in lineage reconstruction from single-cell RNA-sequencing data. *Cell Rep* 34: 108589, 2021.
165. Leopold MD, Obermoser G, Fenwick C, Kleinstuber K, Rashidi N, McNevin JP, Nau AN, Wagar LE, Rozot V, Davis MM, *et al.*: Comparison of CyTOF assays across sites: Results of a six-center pilot study. *J Immunol Methods* 453: 37-43, 2018.
166. Lacinski RA, Dziadowicz SA, Roth CA, Ma L, Melemai VK, Fitzpatrick B, Chaharbakhshi E, Heim T, Lohse I, Schoedel KE, *et al.*: Spatial multiplexed immunofluorescence analysis reveals coordinated cellular networks associated with overall survival in metastatic osteosarcoma. *Bone Res* 12: 55, 2024.
167. Krieg C, Nowicka M, Guglietta S, Schindler S, Hartmann FJ, Weber LM, Dummer R, Robinson MD, Levesque MP, Becher B, *et al.*: High-dimensional single-cell analysis predicts response to anti-PD-1 immunotherapy. *Nat Med* 24: 144-153, 2018.
168. Jiang Y, Wang J, Sun M, Zuo D, Wang H, Shen J, Jiang W, Mu H, Ma X, Yin F, *et al.*: Multi-omics analysis identifies osteosarcoma subtypes with distinct prognosis indicating stratified treatment. *Nat Commun* 13: 7207, 2022.
169. Keung EZ, Burgess M, Salazar R, Parra ER, Rodrigues-Canales J, Bolejack V, Van Tine BA, Schuetze SM, Attia S, Riedel RF, *et al.*: Correlative analyses of the SARCO28 trial reveal an association between sarcoma-associated immune infiltrate and response to pembrolizumab. *Clin Cancer Res* 26: 1258-1266, 2020.
170. Gu L, Peng C, Liang Q, Huang Q, Lv D, Zhao H, Zhang Q, Zhang Y, Zhang P, Li S, *et al.*: Neoadjuvant toripalimab plus axitinib for clear cell renal cell carcinoma with inferior vena cava tumor thrombus: NEOTAX, a phase 2 study. *Signal Transduct Target Ther* 9: 264, 2024.
171. Brekken C, Bruland ØS and de Lange Davies C: Interstitial fluid pressure in human osteosarcoma xenografts: Significance of implantation site and the response to intratumoral injection of hyaluronidase. *Anticancer Res* 20: 3503-3512, 2000.
172. Wu H, Luo Y, Xu D, Ke X and Ci T: Low molecular weight heparin modified bone targeting liposomes for orthotopic osteosarcoma and breast cancer bone metastatic tumors. *Int J Biol Macromol* 164: 2583-2597, 2020.
173. Meng H, Mai WX, Zhang H, Xue M, Xia T, Lin S, Wang X, Zhao Y, Ji Z, Zink JI and Nel AE: Codelivery of an optimal drug/siRNA combination using mesoporous silica nanoparticles to overcome drug resistance in breast cancer in vitro and in vivo. *ACS Nano* 7: 994-1005, 2013.
174. Kontulainen SA, Macdonald HM and McKay HA: Change in cortical bone density and its distribution differs between boys and girls during puberty. *J Clin Endocrinol Metab* 91: 2555-2561, 2006.
175. Dai XM, Ryan GR, Hapel AJ, Dominguez MG, Russell RG, Kapp S, Sylvestre V and Stanley ER: Targeted disruption of the mouse colony-stimulating factor 1 receptor gene results in osteopetrosis, mononuclear phagocyte deficiency, increased primitive progenitor cell frequencies, and reproductive defects. *Blood* 99: 111-120, 2002.
176. Joseph GJ, Vecchi Iii LA, Uppuganti S, Kane JF, Durdan M, Hill P, McAdoo AG, Tanaka H, Kell D, Searcy MB, *et al.*: Programmed cell death protein 1 (PD-1) blockade regulates skeletal remodeling in a sex- and age-dependent manner. *J Bone Miner Res* 40: 950-964, 2025.
177. DeSelm C, Palomba ML, Yahalom J, Hamieh M, Eyquem J, Rajasekhar VK and Sadelain M: Low-dose radiation conditioning enables CAR T cells to mitigate antigen escape. *Mol Ther* 26: 2542-2552, 2018.
178. Yu D, Kahen E, Cubitt CL, McGuire J, Kreahling J, Lee J, Altiock S, Lynch CC, Sullivan DM and Reed DR: Identification of synergistic, clinically achievable, combination therapies for osteosarcoma. *Sci Rep* 5: 16991, 2015.
179. Gargett T, Ebert LM, Truong NTH, Kollis PM, Sedivakova K, Yu W, Yeo ECF, Wittwer NL, Gliddon BL, Tea MN, *et al.*: GD2-targeting CAR-T cells enhanced by transgenic IL-15 expression are an effective and clinically feasible therapy for glioblastoma. *J Immunother Cancer* 10: e005187, 2022.
180. Rahouma M, Karim NA, Baudo M, Yahia M, Kamel M, Eldessouki I, Abouarab A, Saad I, Elmously A, Gray KD, *et al.*: Cardiotoxicity with immune system targeting drugs: A meta-analysis of anti-PD/PD-L1 immunotherapy randomized clinical trials. *Immunotherapy* 11: 725-735, 2019.

